mentary Appendix). A yeast *coq2*-null mutant, the BY4741Δ*coq2* strain, was transformed with pAUR123 (Takara Bio) containing the nonmutated or mutated human *COQ2* cDNA. We measured the growth rate in a medium with a nonfermentable carbon source by monitoring the optical density of a sample measured at a wavelength of 600 nm (OD_{600}). We used mitochondrial fractions prepared from lymphoblastoid cell lines with the QProteome Mitochondria Isolation Kit (Qiagen) as the enzyme source. COQ2 activity (Enzyme Commission number, 2.5.1.39) was assayed as described previously.[20]

COENZYME Q_{10} LEVEL IN TISSUES

Using high-performance liquid chromatography, we measured levels of coenzyme Q_{10} (ubiquinone-10 and ubiquinol-10) and free (unesterified) cholesterol in lymphoblastoid cell lines established from 152 patients with multiple-system atrophy and 76 controls and in cerebellum samples obtained on autopsy from 3 patients with multiple-system atrophy and 3 controls.[21]

STATISTICAL ANALYSIS

All results are presented as means and standard deviations. We used Student's t-test to evaluate the significance of differences in the mean age at disease onset between carriers and noncarriers of the *COQ2* mutation. We used Fisher's exact test to calculate the significance of the difference in allele frequencies between carriers and noncarriers, with contingency tables and standard methods used to compute odds ratios and corresponding 95% confidence intervals. We used the Kruskal–Wallis test, followed by the Steel test, to perform an analysis of variance. All statistical tests were two-sided, and a P value of less than 0.05 was considered to indicate statistical significance.

RESULTS

LINKAGE ANALYSIS OF FAMILIAL DISEASE

Parametric linkage analysis of the six family pedigrees revealed no single locus showing a linkage compatible with autosomal recessive inheritance. However, in the parametric linkage analysis allowing for heterogeneity, we detected several loci showing positive scores for heterogeneity logarithm of the odds (HLOD), indicating that more than one locus was involved in the different multiplex families (Fig. S1B in the Supplementary Appendix). In particular, two regions on chromosome 4 showed the highest HLOD scores, exceeding 2.0. Results of nonparametric linkage analysis (Fig. S1C in the Supplementary Appendix) were consistent with those of parametric linkage analysis allowing for heterogeneity. Parametric linkage analysis of chromosome 4 in individual pedigrees revealed positive LOD scores in an overlapping region in four families (Family 1, Family 2, Family 4, and Family 12), with Family 1 having the highest LOD score of 1.93 (72.795 to 89.616 Mb) (Fig. S1A and S2A in the Supplementary Appendix). Thus, we selected Family 1 to undergo whole-genome sequencing.

SUSCEPTIBILITY GENE IN FAMILIAL DISEASE

Whole-genome sequencing of a sample obtained from Participant II-4, one of two affected members of Family 1, generated 187.5 Gb of short reads, with an average coverage of 58× and 3,492,429 single-nucleotide variants (SNVs) or insertions or deletions. We winnowed the 3,492,429 variants down to 4 by selecting SNVs that were located in the candidate regions defined on linkage analysis in Family 1 (regions with the highest LOD score spanning approximately 80 Mb in total), that were located in exons or splice sites, that were predicted to cause amino acid changes or changes in pre-messenger RNA splicing, and that were not registered in the database of single-nucleotide polymorphisms, build 130 (dbSNP130), indicating that the variants are extremely rare in the general population (Fig. S2B in the Supplementary Appendix). Each of these 4 SNVs is predicted to result in an amino acid substitution: K707R in SHROOM3 (Universal Protein Resource [UniProt] accession number, Q8TF72), M78V and V343A in COQ2 (UniProt accession number, Q96H96), and R231G in SCEL (UniProt accession number, O95171).

In the 180 Japanese control samples, we did not observe the SNV encoding the M78V variant but did observe SNVs encoding K706R in SHROOM3, V343A in COQ2, and R231G in SCEL, which were present on 3, 5, and 98 of 360 alleles, respectively. We therefore considered the SNP encoding M78V in *COQ2*, which encodes parahydroxybenzoate-polyprenyl transferase, an enzyme involved in the biosynthesis of coenzyme Q_{10}, as a candidate variant in conferring susceptibility to familial multiple-system atrophy.

Cosegregation analysis of samples from Family 1 revealed that the two affected family members, Participants II-4 and II-8, carried the homozygous M78V-V343A variant in *COQ2*, and the unaffected sibling who was tested (Participant II-7) did not carry this variant (Fig. S2C in the Supplementary Appendix). Mutational analysis of *COQ2* in Family 12 revealed heterozygous mutations consisting of nonsense (R337X) and missense (V343A) variants in both affected siblings (Participants II-3 and II-4). Their mother (Participant I-2) was heterozygous for V343A, one unaffected sibling (Participant II-1) lacked this variant, and the other unaffected sibling (Participant II-2) was heterozygous for R337X. R337X was not observed in the 180 Japanese controls.

We did not detect variants of *COQ2* in the other four families (Families 2, 3, 4, and 8). Because *COQ2* encodes an enzyme essential for the biosynthesis of coenzyme Q_{10}, we further sequenced the other 11 genes in the biosynthetic pathway for coenzyme Q_{10} (*PDSS1*, *PDSS2*, *COQ3*, *COQ4*, *COQ5*, *COQ6*, *COQ7*, *ADCK3*, *COQ9*, *COQ10A*, and *COQ10B*) in the remaining four families and in a previously described multiplex family[14] but did not observe variants that cosegregated with disease.

COQ2 VARIANTS AND SPORADIC DISEASE

To investigate the involvement of *COQ2* variants in sporadic multiple-system atrophy, we extended the mutational analysis of *COQ2* to a Japanese series consisting of 363 patients with multiple-system atrophy and 520 controls. A common *COQ2* variant (rs6818847, predicted to result in an amino acid substitution, L16V) with allele frequencies of 0.90 and 0.88 in the Japanese patients with multiple-system atrophy and controls, respectively, was not included in further analysis. Four patients with multiple-system atrophy carried two variants simultaneously (one carried an I97T and a nonmutated [NM] allele at codon 97 and V343A/NM at codon 343, one had R337Q/NM at codon 337 and V343A/NM at codon 343, and two had V343A/V343A), whereas none of the controls had two variants of *COQ2* (Table 1). Sequencing of the subcloned mutated alleles confirmed that R337Q/V343A was present in a compound heterozygous state. We were unable to determine the phase of I97T/V343A, because the distance

Table 1. *COQ2* Variants Found in Patients with Sporadic Multiple-System Atrophy in Japanese, European, and North American Series, as Compared with Controls.*

Genotype	Japanese Series		European Series		North American Series	
	Patients (N=363)	Controls (N=520)	Patients (N=223)	Controls (N=315)	Patients (N=172)	Controls (N=294)
P22L/NM	0	1	0	0	0	0
F29L/NM	0	0	1	0	0	0
P49H†/NM	0	0	0	0	1	0
S57T†/NM	0	0	1	0	0	0
R69H†/NM	0	0	0	0	0	1
I97T‡/V343A§	1	0	0	0	0	0
P107S†/NM	1	0	0	0	0	0
S113F†/NM	1	0	0	0	0	0
T267A‡/NM	0	0	1	0	0	0
S297C‡/NM	0	0	1	0	0	0
N336H/NM	0	1	0	0	0	0
R337Q†/V343A§	1	0	0	0	0	0
V343A§/NM	29	17	0	0	0	0
V343A§/V343A§	2	0	0	0	0	0

* NM denotes nonmutated.
† This variant was deemed to be severely deleterious on yeast complementation assay.
‡ This variant was deemed to be mildly deleterious on yeast complementation assay.
§ This variant had decreased COQ2 activity on enzyme assay.

Table 2. Association between the *COQ2* V343A Variant and Sporadic Multiple-System Atrophy in the Japanese Series.*

V343A Variant†	Patients with Multiple-System Atrophy							Patients with Other Neurologic Diseases		
	Patients (N=363)	Tier 1 Controls (N=520)	Comparison with Tier 1		Tier 2 Controls (N=2383)	Comparison with Tier 2		Alzheimer's Disease (N=2728)	Parkinson's Disease (N=659)	ALS (N=634)
			odds ratio (95% CI)	*P value*		*odds ratio (95% CI)*	*P value*			
Allele frequency — no./total no. (%)	35/726 (4.8)	17/1040 (1.6)	3.05 (1.65–5.85)	1.5×10^{-4}	106/4766 (2.2)	2.23 (1.46–3.32)	6.0×10^{-5}	109/5456 (2.0)	33/1318 (2.5)	31/1268 (2.4)
Heterozygous — no.	31	17			106			105	33	31
Homozygous — no.	2	0			0			2	0	0

* Odds ratios and P values are for the comparisons between patients with multiple-system atrophy and each of the two groups of controls (tier 1 and tier 2). ALS denotes amyotrophic lateral sclerosis, and CI confidence interval.

† In the combined series of Japanese, European, and North American participants, functionally deleterious variants P49H, S57T, R69H, I97T, P107S, S113F, T267A, S297C, and R337Q (as determined on yeast complementation assay) were found in 8 of 1516 alleles (0.53%) in patients with multiple-system atrophy, as compared with 1 of 2258 alleles (0.05%) in controls (odds ratio, 11.97; 95% CI, 1.60 to 531.5; P=0.004).

between I97T and V343A was too large to be amplified by means of polymerase-chain-reaction (PCR) assay in a single fragment, and samples of genomic DNA from the parents were unavailable. We found that 29 patients with multiple-system atrophy and 17 controls were heterozygous for the V343A variant. In addition, we detected four novel heterozygous variants: two in patients with multiple-system atrophy (P107S and S113F) and two in controls (P22L and N336H).

Of the *COQ2* variants, the V343A variant is relatively common in the Japanese population. As shown in Table 2, we found that the V343A allele occurred in 35 of 726 alleles (4.8%) from Japanese patients with multiple-system atrophy and in 17 of 1040 alleles (1.6%) from Japanese controls (odds ratio for patients with multiple-system atrophy, 3.05; 95% confidence interval [CI], 1.65 to 5.85; $P=1.5\times10^{-4}$). Genotyping in the second series of 2383 Japanese controls showed that the V343A variant had an allele frequency of 2.2% (106 of 4766 alleles; odds ratio, 2.23; 95% CI, 1.46 to 3.32; $P=6.0\times10^{-5}$). Genotyping Japanese persons with other neurodegenerative diseases revealed that the V343A allele frequencies were 2.0% (109 of 5456 alleles) among patients with Alzheimer's disease, 2.5% (33 of 1318 alleles) among those with Parkinson's disease, and 2.4% (31 of 1268 alleles) among those with ALS. These allele frequencies did not differ significantly from those in the first or second set of controls, confirming the specificity of the V343A variant in patients with multiple-system atrophy. Two patients with Alzheimer's disease who were found to carry homozygous V343A mutations did not show any signs of parkinsonism, cerebellar ataxia, or autonomic dysfunction.

We then performed genotyping in the European and North American series of patients with multiple-system atrophy. In the European series, we found four singleton *COQ2* variants (encoding amino acid substitutions F29L, S57T, T267A, and S297C) among the patients, whereas none of the controls had any variants in *COQ2*. In the North American series, we found one variant (P49H) in a patient with multiple-system atrophy and one variant (R69H) in a control (Table 1). At the time of recruitment for the study, the carrier of R69H, who was 60 years old, had no signs of parkinsonism, cerebellar ataxia, or autonomic dysfunction, but this participant was unavailable for follow-up assessment. Intriguingly, the V343A

variant, a relatively common variant in the Japanese population, was not observed in patients with multiple-system atrophy or controls in either the European or the North American series.

FUNCTIONAL ANALYSIS OF MUTANT *COQ2*

To determine the functional effect of each variant on the mitochondrial aerobic energy production in which coenzyme Q_{10} plays an essential

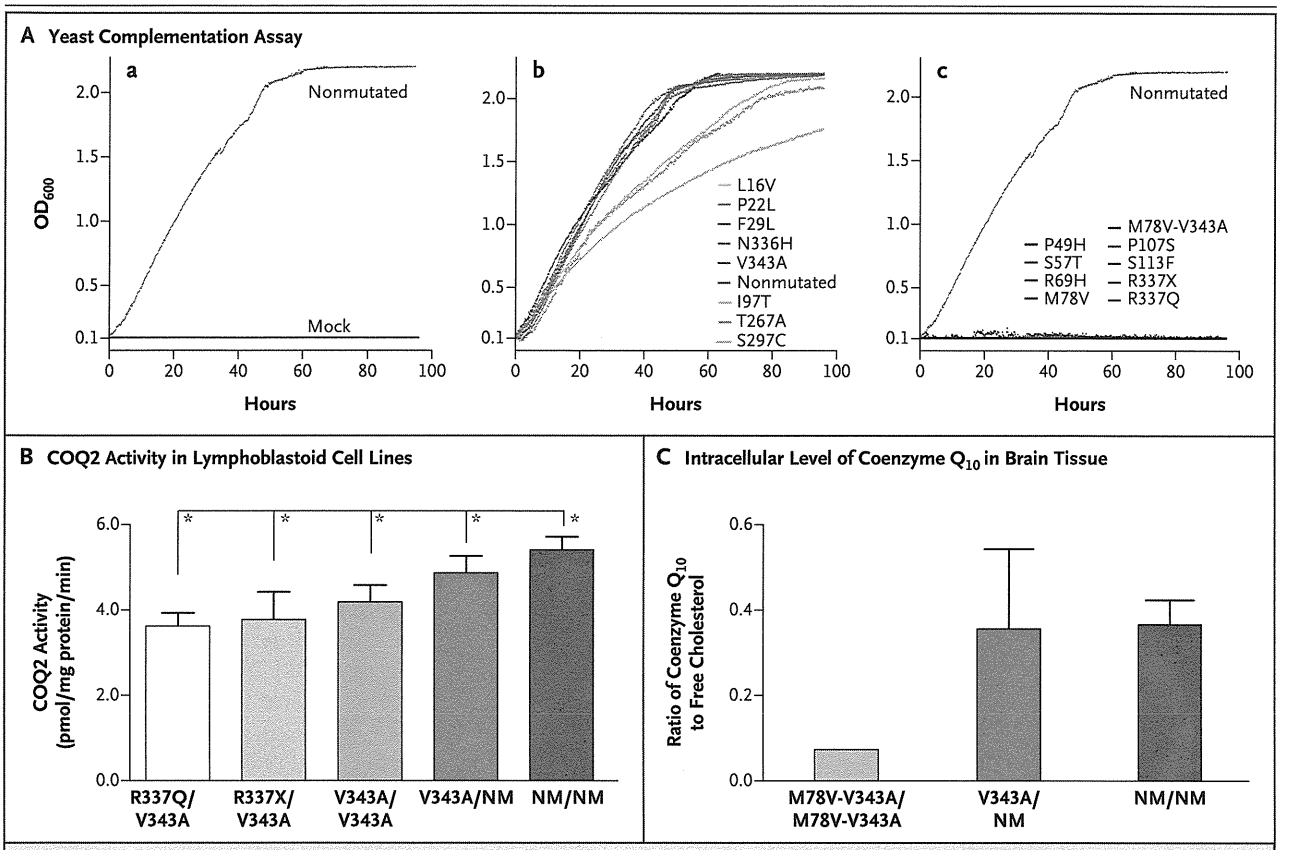

Figure 2. Functional Analysis of *COQ2* Variants.

Panel A shows the results of a yeast complementation assay, including the growth curves of the yeast *coq2*-null mutants transformed with the pAUR123 vector containing the nonmutated (NM) human *COQ2* complementary DNA (cDNA) or mock vector (subpanel a) and those transformed with the AUR123 vector containing different versions of human *COQ2* cDNA (encoding the substitutions L16V, P22L, F29L, N336H, V343A, I97T, T257A, and S297C) (subpanel b). Transformants carrying a *COQ2* allele encoding the I97T, T267A, or S297C substitution show considerably lower growth rates than nonmutated *COQ2*, which still shows a higher growth rate than the *coq2*-null strain (mildly deleterious). Transformants carrying a *COQ2* allele encoding the L16V, P22L, F29L, N336H, or V343A substitution show growth rates similar to that of nonmutated *COQ2*. The *coq2*-null mutants transformed with the pAUR123 vector containing different versions of human *COQ2* cDNA (P49H, S57T, R69H, M78V, M78V-V343A, P107S, S113F, R337X, or R337Q) show severely decreased respiration-dependent growth rates, as does the *coq2*-null strain (severely deleterious) (subpanel c). Each yeast strain was pregrown in yeast extract peptone dextrose (YPD) medium, diluted to an optical density of a sample measured at a wavelength of 600 nm (OD_{600}) of 0.1, and then incubated in yeast extract peptone glycerol (YPG) medium at 23°C with shaking at a rate of 200 rotations per minute for 4 days. OD_{600} was measured every 10 minutes. The experiments were conducted in quadruplicate, and the mean OD_{600} was plotted against the incubation time. Panel B shows COQ2 activity in lymphoblastoid cell lines, as determined by measuring the incorporation of radioactive parahydroxybenzoate (PHB) into decaprenyl-PHB. COQ2 activity was measured in lymphoblastoid cell lines from each patient with multiple-system atrophy carrying *COQ2* variants (encoding R337Q/V343A, R337X/V343A, V343A/V343A, or V343A/NM) and from a control without variants. The mean values from nine independent experiments are shown. T bars indicate standard deviations. Group comparisons were performed with the use of the Kruskal–Wallis test, followed by the Steel test. Asterisks indicate $P<0.05$ for the comparison with a control sample (nonmutated *COQ2* genotype). Panel C shows intracellular levels of coenzyme Q_{10} in frozen cerebellum samples obtained from three patients with multiple-system atrophy (one who was homozygous for M78V-V343A and two who were heterozygous for V343A) and from three controls. Brain-tissue samples weighing approximately 100 mg were homogenized in 10 volumes (volume to weight) of 10 mM TRIS–hydrochloric acid (with a pH of 7.4) containing 0.32 M sucrose, 1 mM ethylenediaminetetraacetic acid (EDTA), and 20% sodium dodecyl sulfate (SDS). Coenzyme Q_{10} was then extracted with hexane and ethanol (in a 5:2 ratio according to volume), and the extract was subjected to high-performance liquid chromatography to measure the level of coenzyme Q_{10}, after adjustment for the free (unesterified) cholesterol level.[21]

role in the electron transfer, we carried out functional complementation analysis by transforming the yeast *coq2*-null strain with nonmutated or mutated human *COQ2* cDNA (Fig. 2A). Transformants of the BY4741 Δ*coq2* yeast strain with the mutated *COQ2*, including transformants separately carrying the P49H, S57T, R69H, M78V, M78V-V343A, P107S, S113F, R337Q, and R337X alleles, showed severely decreased growth rates, similar to those observed in the *coq2*-null strain. In addition, transformants with mutated *COQ2*, including those with the variants encoding the I97T, T267A, and S297C substitutions, showed substantially lower growth rates than those expressing nonmutated *COQ2*, which had a higher growth rate than the *coq2*-null strain (mildly deleterious). The transformants with mutated *COQ2*, including transformants separately carrying the L16V, P22L, F29L, N336H, and V343A alleles, showed growth rates similar to those of the transformants expressing nonmutated *COQ2*. As described above, the yeast strain with M78V-V343A identified in Family 1 showed a severely decreased growth rate, whereas the strain with V343A had a growth rate similar to that of nonmutated *COQ2*, indicating that of the two variants, M78V primarily contributed to the impairment in COQ2 function.

Focusing on the rare variants that were identified in the case–control series (Table 1), we found that nine variants (P49H, S57T, R69H, I97T, P107S, S113F, T267A, S297C, and R337Q) were mildly or severely deleterious. On combining all three series, eight variants (P49H, S57T, I97T, P107S, S113F, T267A, S297C, and R337Q) were identified in 758 patients with multiple-system atrophy, whereas only one variant (R69H) was found in 1129 controls (odds ratio, 11.97; 95% CI, 1.60 to 531.52; P=0.004) (Table 2 footnote). Yeast complementation analysis showed that the F29L variant, identified in a European patient with multiple-system atrophy, did not impair the growth rate. Lymphoblastoid cell lines from this patient were unavailable for further measurement of the activity of mutant COQ2, thus making it difficult to interpret the pathogenicity of this variant.

COQ2 ACTIVITIES IN LYMPHOBLASTOID CELL LINES

We measured COQ2 activities in lymphoblastoid cell lines from patients carrying *COQ2* mutations, when available. We focused on the V343A variant because it is commonly associated with multiple-system atrophy and showed an apparently normal growth rate in the yeast complementation assay. We determined COQ2 activities in lymphoblastoid cell lines with *COQ2* variants R337Q/V343A, R337X/V343A, V343A/V343A, or V343A/NM and in a control without variants. The COQ2 activities in the lymphoblastoid cell lines (V343A/NM) obtained from patients with multiple-system atrophy were significantly lower than those in the control cell lines. The COQ2 activities in the cell lines from patients with multiple-system atrophy carrying two mutated *COQ2* alleles were further decreased (Fig. 2B).

CORRELATIONS BETWEEN GENOTYPE AND PHENOTYPE

The clinical features of patients with sporadic multiple-system atrophy carrying deleterious *COQ2* variants (as determined on yeast complementation assay and COQ2-activity measurement) and those of noncarriers are summarized in Table S5 in the Supplementary Appendix. The mean age at the onset of multiple-system atrophy among carriers was older than that among noncarriers (P=0.002). Among carriers, 34 had subtype C and 5 had subtype P. Among noncarriers, 468 had subtype C and 209 had subtype P. The subtype was unclassified in 42 noncarriers. The ratio of the number of patients with subtype C to the number with subtype P was significantly higher among carriers of *COQ2* variants than among noncarriers (P=0.02).

INTRACELLULAR COENZYME Q_{10} IN LYMPHOBLASTOID CELL LINES

We measured intracellular coenzyme Q_{10} levels in lymphoblastoid cell lines from patients with multiple-system atrophy and controls. The participants were grouped as follows: 3 patients with multiple-system atrophy carrying two variants (R337Q/V343A, R337X/V343A, and V343A/V343A), 16 patients carrying heterozygous V343A, 133 patients without variants, and 76 controls without *COQ2* variants (Table 3). Intracellular levels of coenzyme Q_{10} in lymphoblastoid cell lines from patients with multiple-system atrophy who carried two variant alleles were substantially lower than levels in cell lines from controls without variants. Intracellular coenzyme Q_{10} levels in patients who were heterozygous for V343A and in those without *COQ2* variants were not significantly lower than levels in controls without *COQ2* variants.

Table 3. Intracellular Levels of Coenzyme Q_{10} in Lymphoblastoid Cell Lines, According to *COQ2* Variant.*

Variable	Patients with Multiple-System Atrophy					Controls
	R337Q/V343A	R337X/V343A	V343A/V343A	V343A/NM	NM/NM	NM/NM
No. of participants with variant	1	1	1	16	133	76
Ratio of coenzyme Q_{10} to free (unesterified) cholesterol†	2.19	2.58	1.86	3.38±0.53	3.41±0.74	3.48±0.75
Coenzyme Q_{10} level as a percentage of mean value in controls — %‡	62.9	74.1	53.4	97.1	98.0	100.0

* Plus–minus values are means ±SD. NM denotes nonmutated.

† The ratio of coenzyme Q_{10} to free (unesterified) cholesterol reflects the intracellular level of coenzyme Q_{10}. Lower values indicate decreased levels of intracellular coenzyme Q_{10}, presumably reflecting decreased biosynthesis of coenzyme Q_{10}. To calculate the ratio, coenzyme Q_{10} was measured in nanomoles per liter and free cholesterol in micromoles per liter.

‡ Lower values indicate decreased levels of intracellular coenzyme Q_{10}, as compared with the mean value in controls, presumably reflecting decreased biosynthesis of coenzyme Q_{10}.

COENZYME Q_{10} IN BRAIN TISSUE

Only a limited number of brain-tissue samples from patients with multiple-system atrophy carrying *COQ2* variants were available. Nevertheless, we measured coenzyme Q_{10} in frozen brain tissues from three patients with *COQ2* variants (one patient who was homozygous for M78V-V343A and two patients with V343A/NM) and from three controls without *COQ2* variants (Fig. 2C). The levels of coenzyme Q_{10} in patients who were homozygous for M78V-V343A were substantially lower than the levels in controls.

DISCUSSION

We identified homozygous or compound heterozygous *COQ2* mutations in two of the six multiplex families with multiple-system atrophy, a finding that suggests a role of these mutations in the pathogenesis of familial disease. We further found that functionally impaired variants in *COQ2* were associated with an increased risk of sporadic disease. In familial cases of multiple-system atrophy, linkage analysis strongly indicated locus heterogeneity in these families, and the identification of the causal variants in the remaining four families will require analyses such as whole-genome sequencing.

We found that a common variant (V343A) and multiple rare variants in *COQ2* were associated with sporadic multiple-system atrophy. The V343A variant was found exclusively in the Japanese participants, with an allele frequency of 1.6 to 2.2%. The allele frequency of V343A in patients with multiple-system atrophy (4.8%) was significantly higher than that in controls (1.6 to 2.2%) with odds ratios of 2.23 to 3.05. The modest risk of multiple-system atrophy that was associated with the common variant V343A suggests that V343A is a susceptibility factor rather than a causal factor for this disease. The odds ratio for the presence of deleterious rare variants was 11.97, which is much larger than that for V343A. Nonetheless, we should consider that these heterozygous variants in *COQ2* are not necessarily causal but rather confer a strong susceptibility to sporadic multiple-system atrophy. Members of Family 1 and Family 12 who carried deleterious variants in the heterozygous state did not have clinical signs of multiple-system atrophy.

The ratio of patients with subtype C multiple-system atrophy to those with subtype P was higher among carriers of deleterious *COQ2* variants than among noncarriers, which suggests that the cerebellum is more vulnerable to compromised COQ2 function than other regions of the central nervous system. Of the *COQ2* variants that we detected, the V343A variant was the most prevalent and was exclusively found in Japanese participants. These findings may in part explain the clinical observations that subtype C is more prevalent than subtype P in the Japanese population[9] but not in the European population[11] or the North American population.[12] However, there were only 35 carriers of deleterious *COQ2* variants among 363 patients with multiple-system atrophy in the Japanese case series. In addition, the clinical presentations of the two patients with familial

disease who had the highest mutational load were different: subtype P in the patients in Family 1 and subtype C in the patients in Family 12. Thus, the genotypes of *COQ2* do not fully explain the clinical phenotypes.

Previous studies have shown evidence of mitochondrial respiratory-chain dysfunction or oxidative injury in patients with multiple-system atrophy.[22-24] The combination of oxidative stress and overexpression of oligodendroglial α-synuclein has been reported to replicate the characteristics of this disease.[25-28] Our findings suggest that impaired COQ2 activity, which would be predicted to impair the mitochondrial respiratory chain and increase vulnerability to oxidative stress, causes susceptibility to multiple-system atrophy. A primary deficiency of coenzyme Q_{10} that is caused by *COQ2* mutations has been described as an infantile-onset multisystem disorder and a nephropathy in several families.[29,30] The clinical presentation of these affected family members, however, differed markedly from the presentations of patients with multiple-system atrophy, perhaps because the decrease in COQ2 activity associated with the mutations in patients with multiple-system atrophy appears to be milder than that observed in patients with a primary deficiency of coenzyme Q_{10}.

Previous approaches to identifying susceptibility genes have used genomewide association studies or candidate-gene approaches.[31-33] Our identification of rare *COQ2* variants was accomplished by starting with multiplex families and then extending the analysis to patients with sporadic multiple-system atrophy, reflecting an alternative approach to the elucidation of genetic variants with strong effect sizes in an apparently nongenetic disorder.[34]

From the therapeutic viewpoint, oral supplementation with coenzyme Q_{10} may be helpful in treating multiple-system atrophy, particularly for patients with susceptibility-conferring *COQ2* variants. The safety and side-effect profile of high-dose supplementation with coenzyme Q_{10} have been well established.[35,36]

Supported in part by grants from the Japan Society for the Promotion of Science (KAKENHI) (22129001 and 22129002, to Dr. Tsuji); the Ministry of Health, Labor, and Welfare of Japan (H23-Jitsuyoka [Nanbyo]-Ippan-004, to Dr. Tsuji); the Japanese Ministry of Education, Culture, Sports, Science, and Technology; the French Agency for Research (ANR-09-MNPS-032-01/R09148DS, to Drs. Dürr and Brice); Programme Hospitalier de Recherche Clinique (AOM03059/R05129DD, to Drs. Dürr and Brice); Deutsche Forschungsgemeinschaft (Wu 184-6, to Dr. Wüllner); and Deutsche Parkinson Vereinigung (to Dr. Wüllner).

Disclosure forms provided by the authors are available with the full text of this article at NEJM.org.

We thank the staff members of the Radioisotope Center at the University of Tokyo; Keiko Hirayama, Zhenghong Wu, and Mio Takeyama for their support in laboratory experiments; Dr. Kazuyuki Tao, Shinya Uchino, and Manabu Seki for their technical help; Dr. Cecilia Marelli for her clinical input; Drs. Yoshinori Kajimoto and Kokoro Ozaki for providing DNA samples and clinical information; and the DNA and Cell Bank of Centre de Recherche de l'Institut du Cerveau et de la Moelle Épinière (CRICM) in Paris for technical assistance.

APPENDIX

The members of the Multiple System Atrophy Research Collaboration are as follows: Jun Mitsui, M.D., Ph.D., Takashi Matsukawa, M.D., and Hiroyuki Ishiura, M.D., Ph.D., Department of Neurology, Graduate School of Medicine, University of Tokyo, Tokyo; Yoko Fukuda, Ph.D., Department of Neurology, Graduate School of Medicine, University of Tokyo, Tokyo, and Max-Planck Institute of Immunobiology and Epigenetics, Freiburg, Germany; Yaeko Ichikawa, M.D., Ph.D., Hidetoshi Date, Ph.D., Budrul Ahsan, Ph.D., Yasuo Nakahara, M.D., Ph.D., Yoshio Momose, M.D., Ph.D., Yuji Takahashi, M.D., Ph.D., Atsushi Iwata, M.D., Ph.D., and Jun Goto, M.D., Ph.D., Department of Neurology, Graduate School of Medicine, University of Tokyo, Tokyo; Yorihiro Yamamoto, Ph.D., School of Bioscience and Biotechnology, Tokyo University of Technology, Tokyo; Makiko Komata, Ph.D., and Katsuhiko Shirahige, Ph.D., Center for Epigenetic Disease, Institute of Molecular and Cellular Biosciences, University of Tokyo, Tokyo; Kenju Hara, M.D., Ph.D., Department of Neurology, Brain Research Institute, Niigata University, Niigata, Japan; Akiyoshi Kakita, M.D., Ph.D., Mitsunori Yamada, M.D., Ph.D., and Hitoshi Takahashi, M.D., Ph.D., Department of Pathology, Brain Research Institute, Niigata University, Niigata, Japan; Osamu Onodera, M.D., Ph.D., and Masatoyo Nishizawa, M.D., Ph.D., Department of Neurology, Brain Research Institute, Niigata University, Niigata, Japan; Hiroshi Takashima, M.D., Ph.D., Department of Neurology and Geriatrics, Kagoshima University Graduate School of Medical and Dental Sciences, Kagoshima, Japan; Ryozo Kuwano, M.D., Ph.D., Department of Molecular Genetics, Center for Bioresources, Brain Research Institute, Niigata University, Niigata, Japan; Hirohisa Watanabe, M.D., Ph.D., Mizuki Ito, M.D., Ph.D., and Gen Sobue, M.D., Ph.D., Department of Neurology, Nagoya University Graduate School of Medicine, Nagoya, Japan; Hiroyuki Soma, M.D., Ph.D., Ichiro Yabe, M.D., Ph.D., and Hidenao Sasaki, M.D., Ph.D., Department of Neurology, Hokkaido University Graduate School of Medicine, Sapporo, Japan; Masashi Aoki, M.D., Ph.D., Department of Neurology, Tohoku University School of Medicine, Sendai, Japan; Kinya Ishikawa, M.D., Ph.D., and Hidehiro Mizusawa, M.D., Ph.D., Department of Neurology and Neurological Science, Graduate School of Medical and Dental Science, Tokyo Medical and Dental University, Tokyo; Kazuaki Kanai, M.D., Ph.D., Takamichi Hattori, M.D., Ph.D., and Satoshi Kuwabara, M.D., Ph.D., Department of Neurology, Chiba University School of Medicine, Chiba, Japan; Kimihito Arai, M.D., Ph.D., Division of Neurology, National Hospital Organization, Chiba East Hospital, Chiba, Japan; Shigeru Koyano, M.D., Ph.D., Department of Clinical Neurology and Stroke Medicine, Graduate School of Medicine, Yokohama City University, Yokohama, Japan; Yoshiyuki Kuroiwa, M.D., Ph.D., Department of Neurology, Teikyo University School of Medicine University Hospital, Mizonokuchi, Kawasaki, Japan; Kazuko Hasegawa, M.D., Ph.D., Division of Neurology, National Hospital Organization, Sagamihara National Hospital, Sagamihara, Japan; Tatsuhiko Yuasa, M.D., Ph.D., Department of Neurology, Kama-

gaya-Chiba Medical Center for Intractable Neurological Disease, Kamagaya General Hospital, Chiba, Japan; Kenichi Yasui, M.D., Ph.D., and Kenji Nakashima, M.D., Ph.D., Division of Neurology, Department of Brain and Neurosciences, Faculty of Medicine, Tottori University, Yonago, Japan; Hijiri Ito, M.D., Ph.D., Department of Neurology, Mifukai Vihara Hananosato Hospital, Hiroshima, Japan; Yuishin Izumi, M.D., Ph.D., and Ryuji Kaji, M.D., Ph.D., Department of Clinical Neuroscience, Institute of Health Biosciences, University of Tokushima Graduate School, Tokushima, Japan; Takeo Kato, M.D., Ph.D., Departments of Neurology, Hematology, Metabolism, Endocrinology, and Diabetology, Faculty of Medicine, Yamagata University, Yamagata, Japan; Susumu Kusunoki, M.D., Ph.D., Department of Neurology, Kinki University School of Medicine, Osaka, Japan; Yasushi Osaki, M.D., Ph.D., Department of Geriatrics, Cardiology and Neurology, Kochi Medical School, Nankoku, Japan; Masahiro Horiuchi, M.D., Ph.D., Division of Neurology, Department of Internal Medicine, St. Marianna University School of Medicine, Kawasaki, Japan; Tomoyoshi Kondo, M.D., Ph.D., Department of Neurology, Wakayama Medical University, Wakayama, Japan; Shigeo Murayama, M.D., Ph.D., Department of Neuropathology and the Brain Bank for Aging Research, Tokyo Metropolitan Geriatric Hospital and Institute of Gerontology, Tokyo; Nobutaka Hattori, M.D., Ph.D., Department of Neurology, Juntendo University School of Medicine, Tokyo; Mitsutoshi Yamamoto, M.D., Ph.D., Department of Neurology, Kagawa Prefectural Central Hospital, Takamatsu, Japan; Miho Murata, M.D., Ph.D., Department of Neurology, National Center Hospital of Neurology and Psychiatry, Tokyo; Wataru Satake, M.D., Ph.D., and Tatsushi Toda, M.D., Ph.D., Division of Neurology/Molecular Brain Science, Kobe University Graduate School of Medicine, Kobe, Japan; Alexandra Dürr, M.D., Ph.D., and Alexis Brice, M.D., INSERM, UMR_S975, CRICM, F-75013, Paris, UPMC University of Paris 06, UMR_S975, F-75013, Paris, CNRS UMR 7225, F-75013, Paris, and Hôpital de la Salpêtrière, Département de Génétique et Cytogénétique, F-75013, Paris; Alessandro Filla, M.D., Department of Neurological Sciences, University Federico II, Naples, Italy; Thomas Klockgether, M.D., and Ullrich Wüllner, M.D., Ph.D., Department of Neurology, University of Bonn and German Center for Neurodegenerative Diseases (DZNE), Bonn, Germany; Garth Nicholson, M.B., B.S., Ph.D., University of Sydney at the Australian and New Zealand Army Corps (ANZAC) Research Institute, Concord Hospital, Sydney; Sid Gilman, M.D., Department of Neurology, University of Michigan, Ann Arbor; Clifford W. Shults, M.D.,* Department of Neurosciences, University of California, San Diego, School of Medicine, La Jolla; Caroline M. Tanner, M.D., Ph.D., Parkinson's Institute, Sunnyvale, CA; Walter A. Kukull, M.D., Department of Epidemiology, University of Washington School of Public Health, Seattle; Virginia M.-Y. Lee, Ph.D., Institute on Aging, Udall Parkinson's Research Center, Center for Neurodegenerative Disease Research and the Department of Pathology and Laboratory Medicine, Perelman School of Medicine at the University of Pennsylvania, Philadelphia; Eliezer Masliah, M.D., Department of Neurosciences, University of California San Diego, San Diego; Phillip A. Low, M.D., and Paola Sandroni, M.D., Ph.D., Department of Neurology, Mayo Clinic, Rochester, MN; John Q. Trojanowski, M.D., Ph.D., Institute on Aging, Udall Parkinson's Research Center, Center for Neurodegenerative Disease Research and the Department of Pathology and Laboratory Medicine, Perelman School of Medicine at the University of Pennsylvania, Philadelphia; Laurie Ozelius, Ph.D., Department of Genetics and Genomic Sciences, Mount Sinai School of Medicine, New York; Tatiana Foroud, Ph.D., Department of Medical and Molecular Genetics, Indiana University School of Medicine, Indiana Alcohol Research Center, Indianapolis; and Shoji Tsuji, M.D., Ph.D., Department of Neurology, Graduate School of Medicine and Medical Genome Center, University of Tokyo, Tokyo.

*Deceased.

REFERENCES

1. Graham JG, Oppenheimer DR. Orthostatic hypotension and nicotine sensitivity in a case of multiple system atrophy. J Neurol Neurosurg Psychiatry 1969;32:28-34.
2. Tu PH, Galvin JE, Baba M, et al. Glial cytoplasmic inclusions in white matter oligodendrocytes of multiple system atrophy brains contain insoluble alpha-synuclein. Ann Neurol 1998;44:415-22.
3. Wakabayashi K, Yoshimoto M, Tsuji S, Takahashi H. Alpha-synuclein immunoreactivity in glial cytoplasmic inclusions in multiple system atrophy. Neurosci Lett 1998;249:180-2.
4. Arima K, Uéda K, Sunohara N, et al. NACP/alpha-synuclein immunoreactivity in fibrillary components of neuronal and oligodendroglial cytoplasmic inclusions in the pontine nuclei in multiple system atrophy. Acta Neuropathol 1998;96:439-44.
5. Spillantini MG, Crowther RA, Jakes R, Cairns NJ, Lantos PL, Goedert M. Filamentous alpha-synuclein inclusions link multiple system atrophy with Parkinson's disease and dementia with Lewy bodies. Neurosci Lett 1998;251:205-8.
6. Papp MI, Kahn JE, Lantos PL. Glial cytoplasmic inclusions in the CNS of patients with multiple system atrophy (striatonigral degeneration, olivopontocerebellar atrophy and Shy-Drager syndrome). J Neurol Sci 1989;94:79-100.
7. Nakazato Y, Yamazaki H, Hirato J, Ishida Y, Yamaguchi H. Oligodendroglial microtubular tangles in olivopontocerebellar atrophy. J Neuropathol Exp Neurol 1990;49:521-30.
8. Gilman S, Wenning GK, Low PA, et al. Second consensus statement on the diagnosis of multiple system atrophy. Neurology 2008;71:670-6.
9. Watanabe H, Saito Y, Terao S, et al. Progression and prognosis in multiple system atrophy: an analysis of 230 Japanese patients. Brain 2002;125:1070-83.
10. Tsuji S, Onodera O, Goto J, Nishizawa M. Sporadic ataxias in Japan — a population-based epidemiological study. Cerebellum 2008;7:189-97.
11. Geser F, Seppi K, Stampfer-Kountchev M. The European Multiple System Atrophy-Study Group (EMSA-SG). J Neural Transm 2005;112:1677-86.
12. May S, Gilman S, Sowell BB, et al. Potential outcome measures and trial design issues for multiple system atrophy. Mov Disord 2007;22:2371-7.
13. Hara K, Momose Y, Tokiguchi S, et al. Multiplex families with multiple system atrophy. Arch Neurol 2007;64:545-51.
14. Wüllner U, Schmitt I, Kammal M, Kretzschmar HA, Neumann M. Definite multiple system atrophy in a German family. J Neurol Neurosurg Psychiatry 2009;80:449-50.
15. Hohler AD, Singh VJ. Probable hereditary multiple system atrophy-autonomic (MSA-A) in a family in the United States. J Clin Neurosci 2012;19:479-80.
16. Fukuda Y, Nakahara Y, Date H, et al. SNP HiTLink: a high-throughput linkage analysis system employing dense SNP data. BMC Bioinformatics 2009;10:121.
17. Gudbjartsson DF, Thorvaldsson T, Kong A, Gunnarsson G, Ingolfsdottir A. Allegro version 2. Nat Genet 2005;37:1015-6.
18. Li H, Durbin R. Fast and accurate short read alignment with Burrows-Wheeler transform. Bioinformatics 2009;25:1754-60.
19. Li H, Handsaker B, Wysoker A, et al. The Sequence Alignment/Map format and SAMtools. Bioinformatics 2009;25:2078-9.
20. Burón MI, Hermán MD, Alcaín FJ, Villalba JM. Stimulation of polyprenyl 4-hydroxybenzoate transferase activity by sodium cholate and 3-[(cholamidopropyl) dimethylammonio]-1-propanesulfonate. Anal Biochem 2006;353:15-21.
21. Yamashita S, Yamamoto Y. Simultaneous detection of ubiquinol and ubiquinone in human plasma as a marker of oxidative stress. Anal Biochem 1997;250:66-73.
22. Blin O, Desnuelle C, Rascol O, et al. Mitochondrial respiratory failure in skel-

etal muscle from patients with Parkinson's disease and multiple system atrophy. J Neurol Sci 1994;125:95-101.
23. Martinelli P, Giuliani S, Lodi R, Iotti S, Zaniol P, Barbiroli B. Failure of brain and skeletal muscle energy metabolism in multiple system atrophy shown by in vivo phosphorous MR spectroscopy. Adv Neurol 1996;69:271-7.
24. Yamashita T, Ando Y, Obayashi K, et al. Oxidative injury is present in Purkinje cells in patients with olivopontocerebellar atrophy. J Neurol Sci 2000;175:107-10.
25. Stefanova N, Reindl M, Neumann M, et al. Oxidative stress in transgenic mice with oligodendroglial alpha-synuclein overexpression replicates the characteristic neuropathology of multiple system atrophy. Am J Pathol 2005;166:869-76.
26. Stefanova N, Georgievska B, Eriksson H, Poewe W, Wenning GK. Myeloperoxidase inhibition ameliorates multiple system atrophy-like degeneration in a transgenic mouse model. Neurotox Res 2012; 21:393-404.
27. Ubhi K, Lee PH, Adame A, et al. Mitochondrial inhibitor 3-nitroproprionic acid enhances oxidative modification of alpha-synuclein in a transgenic mouse model of multiple system atrophy. J Neurosci Res 2009;87:2728-39.
28. Ubhi K, Rockenstein E, Mante M, et al. Alpha-synuclein deficient mice are resistant to toxin-induced multiple system atrophy. Neuroreport 2010;21:457-62.
29. López-Martín JM, Salviati L, Trevisson E, et al. Missense mutation of the COQ2 gene causes defects of bioenergetics and de novo pyrimidine synthesis. Hum Mol Genet 2007;16:1091-7.
30. Diomedi-Camassei F, Di Giandomenico S, Santorelli FM, et al. COQ2 nephropathy: a newly described inherited mitochondriopathy with primary renal involvement. J Am Soc Nephrol 2007;18:2773-80.
31. Sasaki H, Emi M, Iijima H, et al. Copy number loss of (src homology 2 domain containing)-transforming protein 2 (SHC2) gene: discordant loss in monozygotic twins and frequent loss in patients with multiple system atrophy. Mol Brain 2011; 4:24.
32. Al-Chalabi A, Dürr A, Wood NW, et al. Genetic variants of the alpha-synuclein gene SNCA are associated with multiple system atrophy. PLoS One 2009;4(9):e7114.
33. Scholz SW, Houlden H, Schulte C, et al. SNCA variants are associated with increased risk for multiple system atrophy. Ann Neurol 2009;65:610-4. [Erratum, Ann Neurol 2010;67:277.]
34. Tsuji S. Genetics of neurodegenerative diseases: insights from high-throughput resequencing. Hum Mol Genet 2010;19: R65-R70.
35. Ferrante KL, Shefner J, Zhang H, et al. Tolerance of high-dose (3,000 mg/day) coenzyme Q10 in ALS. Neurology 2005; 65:1834-6.
36. Hyson HC, Kieburtz K, Shoulson I, et al. Safety and tolerability of high-dosage coenzyme Q10 in Huntington's disease and healthy subjects. Mov Disord 2010; 25:1924-8.

OPEN ACCESS Freely available online

PLOS ONE

TBX1 Mutation Identified by Exome Sequencing in a Japanese Family with 22q11.2 Deletion Syndrome-Like Craniofacial Features and Hypocalcemia

Tsutomu Ogata[1*☯], Tetsuya Niihori[2☯], Noriko Tanaka[3☯], Masahiko Kawai[4], Takeshi Nagashima[5], Ryo Funayama[5], Keiko Nakayama[5], Shinichi Nakashima[1], Fumiko Kato[1], Maki Fukami[6], Yoko Aoki[2], Yoichi Matsubara[2,6]

1 Department of Pediatrics, Hamamatsu University School of Medicine, Hamamatsu, Japan, **2** Department of Medical Genetics, Tohoku University School of Medicine, Sendai, Japan, **3** Department of Pediatrics, Kurashiki Central Hospital, Kurashiki, Japan, **4** Department of Pediatrics, Kyoto University School of Medicine, Kyoto, Japan, **5** Division of Cell Proliferation, United Centers for Advanced Research and Translational Medicine, Tohoku University Graduate School of Medicine, Sendai, Japan, **6** National Research Institute for Child Health and Development, Tokyo, Japan

Abstract

Background: Although *TBX1* mutations have been identified in patients with 22q11.2 deletion syndrome (22q11.2DS)-like phenotypes including characteristic craniofacial features, cardiovascular anomalies, hypoparathyroidism, and thymic hypoplasia, the frequency of *TBX1* mutations remains rare in deletion-negative patients. Thus, it would be reasonable to perform a comprehensive genetic analysis in deletion-negative patients with 22q11.2DS-like phenotypes.

Methodology/Principal Findings: We studied three subjects with craniofacial features and hypocalcemia (group 1), two subjects with craniofacial features alone (group 2), and three subjects with normal phenotype within a single Japanese family. Fluorescence *in situ* hybridization analysis excluded chromosome 22q11.2 deletion, and genomewide array comparative genomic hybridization analysis revealed no copy number change specific to group 1 or groups 1+2. However, exome sequencing identified a heterozygous *TBX1* frameshift mutation (c.1253delA, p.Y418fsX459) specific to groups 1+2, as well as six missense variants and two in-frame microdeletions specific to groups 1+2 and two missense variants specific to group 1. The *TBX1* mutation resided at exon 9C and was predicted to produce a non-functional truncated protein missing the nuclear localization signal and most of the transactivation domain.

Conclusions/Significance: Clinical features in groups 1+2 are well explained by the *TBX1* mutation, while the clinical effects of the remaining variants are largely unknown. Thus, the results exemplify the usefulness of exome sequencing in the identification of disease-causing mutations in familial disorders. Furthermore, the results, in conjunction with the previous data, imply that *TBX1* isoform C is the biologically essential variant and that *TBX1* mutations are associated with a wide phenotypic spectrum, including most of 22q11.2DS phenotypes.

Citation: Ogata T, Niihori T, Tanaka N, Kawai M, Nagashima T, et al. (2014) *TBX1* Mutation Identified by Exome Sequencing in a Japanese Family with 22q11.2 Deletion Syndrome-Like Craniofacial Features and Hypocalcemia. PLoS ONE 9(3): e91598. doi:10.1371/journal.pone.0091598

Editor: Reiner Albert Veitia, Institut Jacques Monod, France

Received November 12, 2013; **Accepted** February 12, 2014; **Published** March 17, 2014

Funding: This work was supported in part by grants from the Ministry of Health, Labor, and Welfare, from the Ministry of Education, Culture, Sports, Science and Technology, and from the National Center for Child Health and Development. The funders had no role in study design, data collection and analysis, decision to publish, or preparation of the manuscript.

Competing Interests: The authors have declared that no competing interests exist.

* E-mail: tomogata@hama-med.ac.jp

☯ These authors contributed equally to this work.

Introduction

Chromosome 22q11.2 deletion syndrome (22q11.2DS) is a developmental disorder associated with characteristic craniofacial features with velopharyngeal incompetence, cardiovascular anomalies primarily affecting the outflow tracts, hypoparathyroidism and resultant hypocalcemia, and thymic hypoplasia leading to susceptibility to infection [1]. This condition is also frequently accompanied by non-specific clinical features such as developmental retardation [1]. Expressivity and penetrance of these features are highly variable and, consistent with this, chromosome 22q11.2 deletions have been identified in DiGeorge syndrome (DGS) and velocardiofacial syndrome (VCFS) with overlapping but different patterns of clinical features [1].

While multiple genes are involved in chromosome 22q11.2 deletions [2], *TBX1* (T-box 1) has been regarded as the major gene relevant to the development of clinical features in 22q11.2DS [3]. Indeed, heterozygous *TBX1* mutations have been identified in several deletion-negative patients with 22q11.2DS phenotype [2–8], and mouse studies argue for the critical role of *Tbx1* in the development of 22q11.2DS phenotypes [3]. However, the frequency of *TBX1* mutations remains rare in deletion-negative patients: Gong et al. identified only a few probable *TBX1* mutations after studying 40 patients with DGS/VCFS phenotypes

[4], and Zweier et al. found a single *TBX1* mutation after examining 10 patients with 22q11.2DS phenotype [8]. This indicates the presence of genetic heterogeneity in the development of 22q11.2DS phenotype in deletion-negative patients. Consistent with this, another DGS/VCFS locus has been assigned to chromosome 10p13-14 region [9]. Thus, it would be reasonable to perform a comprehensive genetic analysis in deletion-negative patients with 22q11.2DS phenotype.

In this regard, recent advance in molecular technologies has enabled to perform comprehensive genetic analyses, thereby contributing to the identification of underlying factors in genetic disorders. Indeed, genomewide array comparative genomic hybridization (CGH) has identified multiple disease-associated copy-number changes [10], and exome sequencing has discovered multiple disease-causing gene mutations [11]. In particular, these technologies can be powerful methods for familial disorders, because it is predicted that a single copy-number change or mutation is shared in common by affected subjects and is absent from non-affected subjects within a family.

Here, we performed array CGH analysis and exome sequencing in a family with 22q11.2DS-like clinical features. Although this study did not discover a novel disease gene, a *TBX1* mutation was successfully identified.

Materials and Methods

Ethics statement

The Institutional Review Board Committees of Hamamatsu University School of Medicine, Tohoku University School of Medicine, Kurashiki Central Hospital, and National Research Institute for Child Health and Development considered and approved the study, consent/assent procedures, and the publication of images and case details associated with this work. The individuals in this manuscript have given written informed consent (as outlined in PLOS consent form) to publish these case details. Actually, this study was performed after obtaining written informed consent from the parents of the child subjects and from the adult subjects. Furthermore, the mother and the elder brother aged 19 years old have given written informed consent to publication of the facial photographs of the two brothers; in addition, the younger brother aged 10 years has given informed assent.

Clinical Report

The pedigree of this Japanese family is shown in Fig. 1, and clinical findings of the family members are summarized in Table 1. The proband (subject III-5) was found to have hypocalcemia and hyperphosphatemia in a pre-operation laboratory test for repeated otitis media at 8 years of age, and was referred to Department of Pediatrics at Kurashiki Central Hospital. Subsequent examination revealed borderline low serum intact PTH value. Thus, he was diagnosed as having hypoparathyroidism, and received vitamin D therapy. Furthermore, physical examination showed characteristic craniofacial features with velopharyngeal incompetence suggestive of 22q11.2DS.

Similar craniofacial features were also exhibited by subjects II-2, III-1, III-6, and III-7, and hypocalcemia was also identified in subjects II-2 and III-7. Actually, subject II-2 was taking vitamin D, and subject III-7 was noticed to have hypocalcemia at birth because of the history of subject III-5, and was treated with vitamin D. The five subjects with 22q11.2DS-like craniofacial features lacked cardiovascular anomalies; while they also lacked susceptibility to infection, except for repeated otitis media in subject III-5, thymic hypoplasia was not evaluated in four of the five subjects. By contrast, the five subjects exhibited borderline to mild developmental delay. Indeed, adult subjects II-2 and III-1 had some difficulty in verbal communications, although they were able to get on their daily life, and subject II-2 was able to take care of family members. Similarly, child subjects III-5, III-6, and III-7 also showed speech delay, and subjects III-5 and III-7 received speech therapy. Furthermore, subject III-7 was diagnosed as having pervasive developmental disorder, and his verbal, performance, and full scale intelligence quotients were assessed as 63, 64, and 60, respectively, by the WISC-III method at 10 years of age. In addition, subject II-2 had sensorineural deafness, and subject III-5 had Graves' disease.

Molecularly Studied Subjects

Molecular studies were performed for eight subjects in this family, using peripheral blood samples. They were divided into three groups in terms of clinical findings: group 1, subjects II-2, III-5, and III-7 with craniofacial features and hypocalcemia; group 2, subjects III-1 and III-6 with craniofacial features alone; and group 3, subjects II-1, III-3, and IV-1 with apparently normal phenotype (Fig. 1).

FISH and Array CGH Analyses

Fluorescence *in situ* hybridization (FISH) analysis was performed with a probe for *HIRA* on the commonly deleted chromosome 22q11.2 region and that for *ARSA* at chromosome 22q13 utilized as an internal control (Abott). Array CGH was carried out using a genomewide 2x400K Agilent platform catalog array, according to the manufacturer's instructions (Agilent Technologies), and copy number variants/polymorphisms were screened with Agilent Genomic Workbench software using the Database of Genomic Variants (http://dgv.tcag.ca/dgv/app/home).

Exome and Sanger Sequencings

Exon capture was performed with the SureSelect Human All Exon kit v4 (Agilent Technologies). Exon libraries were sequenced with the Illumina Hiseq 2000 platform according to the manufacturer's instructions (Illumina), providing 108–122 average depth for each sample. Paired 101-base pair reads were aligned to the reference human genome (UCSChg19) using the Burrows-Wheeler Alignment tool [12]. Likely PCR duplicates were removed with the Picard program (http://picard.sourceforge.net/). Single-nucleotide variants and indels were identified using the Genome Analysis Tool Kit (GATK) v1.6 software [13]. SNVs and indels were annotated against the RefSeq database, 1000 Genomes Project variant data, and dbSNP135 with the ANNOVAR program [14].

To confirm mutations indicated by exome sequencing, Sanger sequencing was performed for PCR products obtained with primers flanking the detected mutations, using a 3500xL genetic analyzer (Life Technologies). Furthermore, the PCR products were subcloned with TOPO TA Cloning Kit (Life Technologies), and normal and mutant alleles were sequenced separately.

In silico protein functional analysis

Function of proteins with missense variations was assessed by Polymorphism Phenotyping-2 (PolyPhen-2, http://genetics.bwh.harvard.edu/pph2/) and Sorting Intolerant From Tolerant (SIFT, http://sift.jcvi.org/), and that of proteins with in-frame amino acid deletions was evaluated by PROVEAN predictions (http://provean.jcvi.org/index.php).

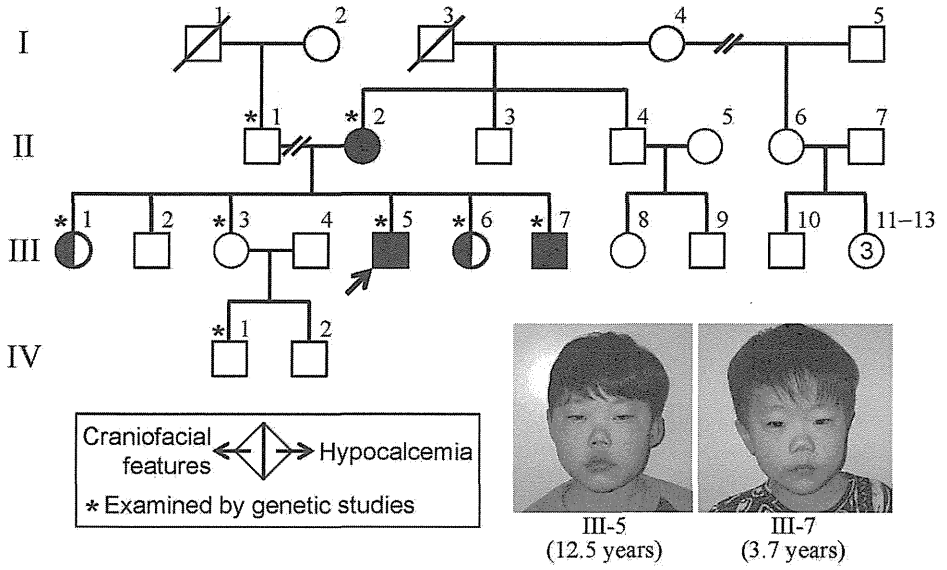

Figure 1. The pedigree of this family. Facial features of subjects III-5 and III-7 are shown.
doi:10.1371/journal.pone.0091598.g001

Results

FISH and Array CGH Analyses

FISH analysis delineated two signals for *HIRA* (Fig. 2A). Array CGH analysis revealed no copy number change specific to group 1 or groups 1+2, in the entire genome including chromosome 10p13-14 and chromosome 22q11.2 regions (Fig. 2B).

Exome and Sanger Sequencings

Exome sequencing identified nine heterozygous non-synonymous variants (six missense variants, two in-frame microdeletions, and one frameshift variant) that were specific to groups 1+2 (namely, they were present in groups 1+2 and absent from group 3 as well as from 1000 Genomes, dbSNP135, and our in-house exome data from 70 individuals) (Table S1). Notably, the frameshift variant (c.1253delA, p.Y418fsX459) was found at exon 9C of *TBX1* for DGS/VCFS (Fig. 3). Of the remaining eight variants, two variants were also detected in disease-related genes: p.G204R in *HDAC4* for brachydactyly-mental retardation syndrome [15], and p.276del in *CCND1* constituting a susceptibility factor for colorectal cancer and a modifier for von Hippel-Lindau disease [16,17]. Exome sequencing also detected two heterozygous missense variants that were specific to group 1 (Table S1).

When all variants were included, exome sequencing revealed: (1) 83 non-synonymous and 86 synonymous variants that were present in groups 1+2 and absent from group 3 (Table S2); (2) 54 non-synonymous and 48 synonymous variants that were present in group 1 and absent from groups 2+3 (Table S3); (3) 6,033 non-synonymous and 6,667 synonymous variants that were present in groups 1+2, but not specific to groups 1+2 (thus, they may be present in group 3 or absent from group 3); and (4) 7,073 non-synonymous and 7,861 synonymous variants that were present in group 1, but not specific to group 1. Furthermore, comparison of the exome sequencing data between group 1 with hypocalcemia and group 2 without hypocalcemia revealed 231 non-synonymous and 254 synonymous variants that were present in group 1 and absent from group 2 (Table S4), and 246 non-synonymous and 242 synonymous variants that were present in group 2 and absent from group 1 (Table S5). (The variant data other than those described in Supplemental Tables may be available on request after discussion with the family members and approval by our IRBs, because they contain a huge amount of individual genetic information.)

In silico protein functional analysis

The results are summarized in Table S1. The p.G204R in *HDAC4* and the p.E276del in *CCND1* were assessed as non-pathologic, while some variants were evaluated as potentially pathologic.

Discussion

Exome sequencing successfully identified a heterozygous frameshift variant on exon 9C of *TBX1*. The c.1253delA (p.Y418fsX459) appears to be a disease-causing mutation, because it is predicted that this variant escapes nonsense-mediated mRNA decay due to its position on the final exon [18] and produces a truncated protein lacking the nuclear localization signal (NLS) and most of the transactivation domain (TAD) on exon 9C (Fig. 3) [19]. In support of this, functional studies for a similar c.1223delC (p.S408fsX459) mutation on exon 9C have shown that the truncated p.S408fsX459 protein was incapable of localizing to nucleus and lost transactivation function [2,5,19]. One may argue that this c.1253delA mutation affects *TBX1* isoform C (*TBX1C*, TBX1-003) alone, while *TBX1* produces three transcript variants containing T-box [2,4] (Fig. 3). However, *TBX1C* is the major transcript with the NLS and the TAD in human and is highly homologous to mouse *Tbx1* [4] (Fig. S1).

Craniofacial features in groups 1+2 and hypocalcemia in group 1 are well explained by the *TBX1* mutation [3]. This argues for a critical role of this mutation in the phenotypic development in groups 1+2, while the clinical effects of the remaining variants identified by exome sequencing are largely unknown. In this regard, comparison between group 1 with hypocalcemia and group 2 without hypocalcemia revealed a large number of non-synonymous and synonymous variants that exclusively belonged to either group 1 (Table S4) or group 2 (Table S5), although the lists did not contain a c.2968A>G (p.R990G) SNP in *CASR* (calcium sensing receptor) that has a gain-of-function effect and appears to raise the susceptibility to hypocalcemia (Fig. S2) [20]. Thus, it is

Table 1. Clinical findings of the family members.

	TBX1 mutation (+)					*TBX1* mutation (−)			*TBX1* mutation (N.E.)		
Individual	**II-2**	**III-1**	**III-5**	**III-6**	**III-7**	**II-1**	**III-3**	**IV-1**	**II-3**	**II-4**	**III-2**
Present age (year)	51	26	19	13	10	59	22	5	50	49	25
Sex	F	F	M	F	M	M	F	M	M	M	M
Craniofacial features	+	+	+	+	+	−	−	−	−	−	−
Hypertelorism	+	+	+	+	+	−	−	−	−	−	−
Blepharophimosis	+	+	+	+	+	−	−	−	−	−	−
Low set ears	+	+	+	+	+	−	−	−	−	−	−
Auricular anomalies	+	−	−	−	−	−	−	−	−	−	−
Narrow nose	+	+	+	+	+	−	−	−	−	−	−
Cleft palate	−	−	−	−	−	−	−	−	−	−	−
Micrognathia	±	+	+	+	+	−	−	−	−	−	−
Velopharyngeal incompetence	+[d]	+	+	+	+	−	−	−	−	−	−
Hypoparathyroidism	+	−	+	−	+	−	−	−	−	−	−
Age at examination (year)	44	17	8	4	0 (1 day)	N.E.	15	0 (6 days)	N.E.	N.E.	18
Serum calcium (mg/dL)[a]	7.6[e]	9.0	6.0	9.1	5.9	...	9.0	9.8	...	...	9.6
Serum i-phosphate (mg/dL)[a]	3.9[e]	4.9	9.1	5.0	N.E.	...	4.8	6.3	...	...	4.6
Serum intact PTH (pg/dL)[a]	31[e]	N.E.	15	N.E.	19	...	N.E.	34	...	...	N.E.
Cardiovascular anomalies[b]	−	−	−	−	−	−	−	−	−	−	−
Hypoplastic thymus[c]	−	N.E.	N.E.	N.E.	N.E.	N.E.	N.E.	N.E.	N.E.	N.E.	N.E.
Susceptible to infection	−	−	−[f]	−	−	−	−	−	−	−	−
Other features	−	−	−	−	−	−	−	−	−	−	−
Developmental retardation	+	+	+[g]	+	+[g]	−	−	−	−	−	−
Sensorineural deafness	+[h]	−	−	−	−	−	−	−	−	−	−
Graves' disease	−	−	+[i]	−	−	−	−	−	−	−	−

Individuals correspond to those shown in Fig. 1.
i-phosphate: inorganic phosphate; SD: standard deviation; F: female; M: male; and N.E.: not examined.
[a]Reference values: calcium, 9.0–11.0 mg/dL in infants and 8.8–10.2 mg/dL in adults; inorganic phosphate, 4.8–7.5 mg/dL in infants and 2.5–4.5 mg/dL in adults, and intact PTH, 10–65 pg/dL in infants and 14–55 pg/dL in adults.
Conversion factor to the SI unit: 0.25 for calcium (mmol/L), 0.32 for inorganic phosphate (mmol/L), and 0.106 for intact PTH (pmol/L).
[b]Examined by echocardiography, chest roentgenography, and/or electrocardiography.
[c]Examined by computed tomography.
[d]Received velopharyngeal closure.
[e]On treatment with vitamin D.
[f]Repeated otitis media only.
[g]Received speech therapy.
[h]Required hearing aids.
[i]At the time of diagnosis (11 years of age), serum TSH was <0.01 mIU/L, free T_3 33.1 pg/mL [51.0 pmol/L], free T_4 5.11 ng/dL [65.8 nmol/L], and TSH receptor antibody 1284% [normal range <1.9%].
doi:10.1371/journal.pone.0091598.t001

likely that, together with environmental factors, the combination of hitherto unknown calcium metabolism-related functional variants would underlie different serum calcium values between groups 1 and 2.

In addition to craniofacial features with and without hypocalcemia, *TBX1* mutation positive subject II-2 had sensorineural deafness, and III-5 had Graves' disease. Since such features are occasionally manifested by patients with 22q11.2DS [21,22], the results may suggest the relevance of *TBX1* to such rather infrequent features in 22q11.2DS.

The five *TBX1* mutation positive subjects in groups 1+2 lacked cardiovascular lesion and manifested borderline to mild developmental retardation (while they had no susceptibility to infection, assessment of thymic hypoplasia remained fragmentary). By contrast, cardiovascular lesion is frequently observed and developmental retardation is rare in previously reported patients with *TBX1* mutations, although clinical features are fairly variable among mutation positive patients (Table 2). Such difference would more or less be ascribed to an examination bias that *TBX1* has been analyzed in patients with isolated cardiovascular lesion in several studies [4,6,7] or to the functional difference of the mutant proteins [2,5–8]. However, in seven patients who have been examined for DGS/VCFS-like clinical features and found to have frameshift mutations on exon 9C (p.S408fsX459, p.H425fsX613, and p.S431fsX608) affecting the NLS and the TAD, cardiovascular lesion was present in four patients and developmental delay was absent or not described, despite apparent similarity in the ascertainment of patients and the function of mutant proteins between the seven patients and the five affected subjects in this family (Table 2) [2–5].

Thus, there may be protective factor(s) for cardiovascular lesion and susceptibility factor(s) for developmental delay in groups 1+2.

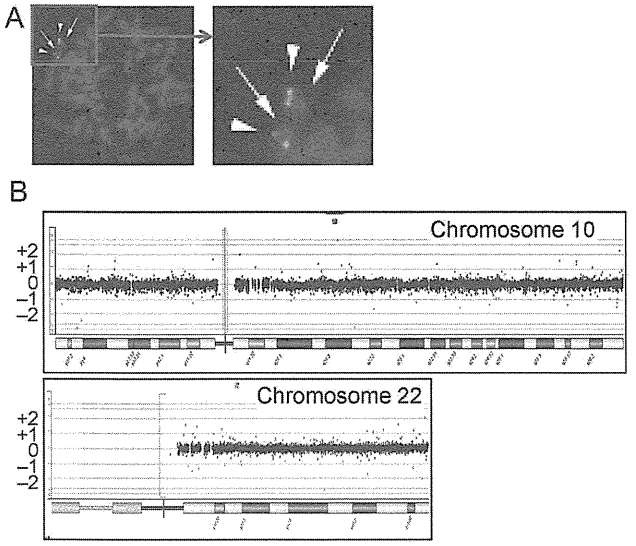

Figure 2. FISH and array CGH analyses in the proband (III-5). A. FISH analysis. Two signals are shown for both *HIRA* at 22q11.2 (red signals indicated by arrows) and *ARSA* at 22q13 (green signals indicated by arrowheads). **B.** Array CGH analysis. No copy number change is found for chromosome 10 carrying the second DiGeorge region and chromosome 22 harboring the DGS/VCFS critical region, as well as other chromosomes (not shown). Black, red, and green dots denote signals indicative of the normal, the increased (>+0.5), and the decreased (<−0.8) copy numbers, respectively. Although several red and green signals are seen, there is no portion associated with ≥3 consecutive red or green signals.
doi:10.1371/journal.pone.0091598.g002

In this regard, a simple explanation would be that protective factor(s) for cardiovascular lesion are present in groups 1+2 and may be present in group 3 or absent from group 3, whereas susceptibility factor(s) for developmental delay is present in groups 1+2 and absent from group 3. Since 6,033 non-synonymous and 6,667 synonymous variants were found to be present in groups 1+2 but not specific to groups 1+2, and 83 non-synonymous and 86 synonymous variants were revealed to be present in groups 1+2 and absent from group 3, a certain fraction of functional variants may constitute protective factor(s) for cardiovascular lesion and susceptibility factor(s) for developmental delay. In addition, while p.G204R on *HDAC4* for brachydactyly-mental retardation syndrome was assessed as non-pathologic by *in silico* analysis, it may have played a certain role in the occurrence of developmental delay in groups 1+2. Actually, such protective and susceptibility factor(s) would be more complex, with the effects of functional variants unique to each patient as well as the influences of environmental factors. Furthermore, it remains possible that the c.1253delA (p.Y418fsX459) mutation found in this study may be related to a specific phenotype characterized by the presence of craniofacial features and developmental delay and by the absence of cardiovascular lesion, because of a hitherto unrevealed mechanism(s). This matter awaits further studies.

Besides the clinical findings, several matters are also notable in the nine apparently pathologic *TBX1* mutations identified to date (Table 2). First, the mutations reside on exons 3–8 common to isoforms A–C or on exon 9C specific to isoform C, with no mutation on exons 9A and 9B specific to isoforms A and B. This would be consistent with *TBX1C* having the primary biological function. Second, while most mutations have loss-of-function effects, gain-of-function effects have been suggested for p.F148Y, p.H194Q, and p.310S by *in vitro* studies [8]. Thus, *TBX1* loss-of-function mutations and gain-of-function mutations may result in overlapping clinical features. Lastly, the c.1274_1281delAC-TATCTC (p.H425fsX613) missing the NLS on exon 9C was shared by a patient with DGS-like phenotype and the apparently normal mother, and the c.129_185del57 (p.43-61del19) with reduced transcriptional activity was common to a patient with non-syndromic tetralogy of Fallot and the apparently normal mother. This would imply the reduced penetrance of phenotypes caused by these mutations.

In summary, we identified a *TBX1* mutation by exome sequencing in a family with chromosome 22q11.2 deletion-like

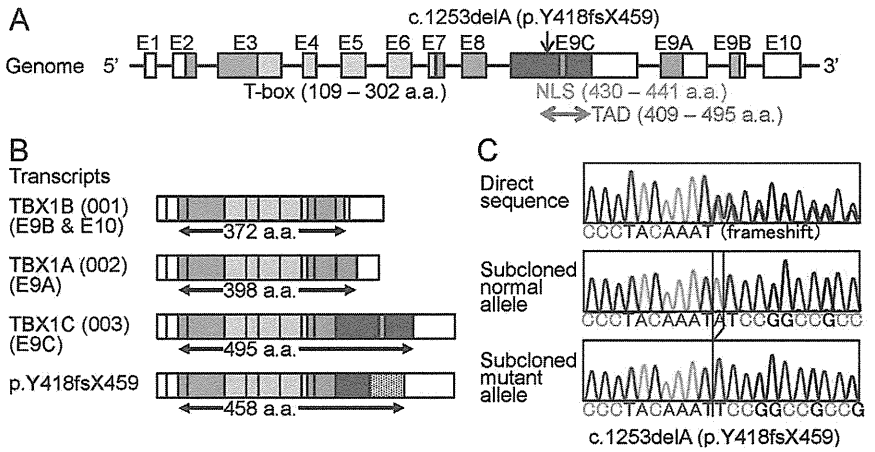

Figure 3. *TBX1* mutation identified in this family. A. Genomic structure of *TBX1* and the position of the mutation. The color and the white boxes represent the coding regions and the untranslated regions on exons 1–10 (E1–E10), respectively; the red, the purple, and the orange segments indicate the coding regions on the final exons 9C, 9A, and 9B (splice variants), respectively. The T-box is indicated by yellow boxes, the nuclear localization signal (NLA) by a blue segment, and the transactivation domain (TAD) by a green arrow. The c.1253delA (p.Y418fsX459) identified in this family resides on exon 9C. **B.** Transcripts of *TBX1*. Three variants are formed by alternative splicing of the final exons 9C, 9A, and 9B. The c.1253delA (p.Y418fsX459) mutation is predicted to yield a truncated TBX1C protein missing the NLS and most of the TAD. The stippled box of p.Y418fsX459 denotes aberrant amino acid sequence produced by the frameshift mutation. **C.** Electrochromatograms showing the frameshift mutation by Sanger sequencing. The primer sequences used are: 5′-GCGGCCAAGAGCCTTCTCT-3′ and 5′-GGGTGGTAGCCGTGGCCA-3′.
doi:10.1371/journal.pone.0091598.g003

Table 2. Summary of patients with *TBX1* mutations.

	TBX1C only					TBX1A–C				22q11.2DS
Position	**Exon 9C**	**Exon 9C**	**Exon 9C**	**Exon 9C**	**Exon 9C**	**Exon 3**	**Exon 4**	**Exon 5**	**Exon 8**	
cDNA change[a]	c.1223	c.1253	c.1274_1281	c.1293_1315	c.1399_1428	c.129_185	c.443T>A	c.582C>G	c.928G>A	Deletion
	delC	delA	del8	del23[h]	dup30[k]	del57[k]				
Amino acid	p.S408	p.Y418	p.H425	p.S431	p.467_476	p.43_61	p.F148Y	p.H194Q	p.G310S	
change	fsX459	fsX459	fsX613	fsX608	dup10A	del19				
NLS (exon 9C)	–	–	–	+[i]	+[l]	+	+	+	+	
TAD (exon 9C)	–	Involved	Involved	Involved	Involved	+	+	+	+	
Function	LOF	N.E.	N.E.	LOF	LOF	Reduced	GOF[m]	GOF[m]	GOF[m]	
Patient number	3	5	1	3[j]	2	1	1	2	1	558
Occurrence	Familial	Familial	Sporadic[g]	Familial	Sporadic	Sporadic[g]	Sporadic	Familial	Sporadic	
Facial features[b]	3/3	5/5	+	3/3	0/2	–	+	2/2	+	100%
Nasal voice[c]	2/3	5/5	N.D.	3/3	0/2	–	+	0/2	+	32%
Cardiovascular anomalies	1/3	0/5	+	2/3	2/2	+	+	0/2	+	57%
Hypopara-thyroidism[d]	1/3	3/5	+	N.D.	0/2	–	–	0/2	+	60%
Hypoplastic thymus	1/2[e]	0/1[f]	+	N.D.	0/2	–	–	N.E.	+	?
Susceptible to infection	N.D.	0/5	N.D.	N.D.	0/2	–	N.D.	N.D.	N.D.	?
Developmental retardation	0/3	5/5	N.D	0/3	0/2	–	–	1/2	–	38%
Reference	2	This study	3, 4	5	4, 6	7	2	8	2	1

In addition to the mutations listed in this table, several missense variants and in-frame indels with unknown functions have been found in patients with isolated cardiovascular anomalies and in those with DGS/VCFS-like phenotype [4].
NLS: nuclear localization signal; TAD: transactivation domain; LOF: loss-of-function; N.D.: not described; N.E.: not examined; GOF: gain-of-function; Del: deletion; and Dup: duplication.
[a]According to NM_080647.
[b]Suggestive of 22q11.2 deletion syndrome.
[c]Velopharygeal insufficiency.
[d]Hypocalcemia is included.
[e]Two of the three subjects have been examined for hypoplastic thymus.
[f]One of the five subjects has been examined for hypoplastic thymus.
[g]These two mutations have been inherited from apparently normal mothers.
[h]The c.1293-1315del23 has been described as c.1320-1342del23 in the original report [5].
[i]Although the natural NLS has been disrupted, a new NLS-compatible motif (RGRRRRCR) has been created on the added amino acid sequence.
[j]Another deceased individual in this family also has similar clinical features.
[k]These two mutations have been identified in *TBX1* analyses for patients with cardiovascular anomalies only.
[l]The mutant protein is aggregated in the cytoplasm and the nucleus.
[m]Gain-of-function effects have been found by *in vitro* studies [8].
doi:10.1371/journal.pone.0091598.t002

phenotype. Application of such powerful methods will serve to identify a causative gene in genetically heterogeneous disorders.

Supporting Information

Figure S1 Comparison of amino acid sequence of human *TBX1C* and mouse *Tbx1*. The T-box is highlighted in yellow, and the nuclear localization signal in light blue. The region for transactivation domain is surrounded by squares. The Y highlighted in red denotes the amino acid residue where the frameshift mutation in this family has taken place.
(TIF)

Figure S2 Analysis of c.2968A>G SNP (p.R990G, rs1042636) with a gain-of-function effect in exon 7 of *CASR*. The SNP pattern is not co-segregated with the presence or absence of hypocalcemia.
(TIF)

Table S1 Summary of heterozygous non-synonymous variants.
(PDF)

Table S2 A list of variants that are present in groups 1+2 and absent from group 3.
(PDF)

Table S3 A list of variants that are present in group 1 and absent from groups 2+3.
(PDF)

Table S4 A list of variants that are present in group 1 and absent from group 2.
(PDF)

Table S5 A list of variants that are present in group 2 and absent from group 1.
(PDF)

References

1. Ryan AK, Goodship JA, Wilson DI, Philip N, Levy A, et al. (1997) Spectrum of clinical features associated with interstitial chromosome 22q11 deletions: a European collaborative study. J Med Genet 34: 798–804.
2. Yagi H, Furutani Y, Hamada H, Sasaki T, Asakawa S, et al. (2003) Role of TBX1 in human del22q11.2 syndrome. Lancet 362: 1366–1373.
3. Baldini A (2005) Dissecting contiguous gene defects: TBX1. Curr Opin Genet Dev 15: 279–84.
4. Gong W, Gottlieb S, Collins J, Blescia A, Dietz H, et al. (2001) Mutation analysis of TBX1 in non-deleted patients with features of DGS/VCFS or isolated cardiovascular defects. J Med Genet 38: E45.
5. Paylor R, Glaser B, Mupo A, Ataliotis P, Spencer C, et al. (2006) Tbx1 haploinsufficiency is linked to behavioral disorders in mice and humans: implications for 22q11 deletion syndrome. Proc Natl Acad Sci U S A 103: 7729–7734.
6. Rauch R, Hofbeck M, Zweier C, Koch A, Zink S, et al. (2010) Comprehensive genotype-phenotype analysis in 230 patients with tetralogy of Fallot. J Med Genet 47: 321–331.
7. Griffin HR, Töpf A, Glen E, Zweier C, Stuart AG, et al. (2010) Systematic survey of variants in TBX1 in non-syndromic tetralogy of Fallot identifies a novel 57 base pair deletion that reduces transcriptional activity but finds no evidence for association with common variants. Heart 96: 1651–1655.
8. Zweier C, Sticht H, Aydin-Yaylagül I, Campbell CE, Rauch A (2007) Human TBX1 missense mutations cause gain of function resulting in the same phenotype as 22q11.2 deletions. Am J Hum Genet 80: 510–517.
9. Daw SCM, Taylor C, Kraman M, Call K, Mao J, et al. (1996) A common region of 10p deleted in DiGeorge and velocardiofacial syndromes. Nat Genet 13: 458–461.
10. McDonnell SK, Riska SM, Klee EW, Thorland EC, Kay NE, et al. (2013) Experimental designs for array comparative genomic hybridization technology. Cytogenet Genome Res 139: 250–257.
11. Wang Z, Liu X, Yang B-Z, Gelernter J (2013) The role and challenges of exome sequencing in studies of human diseases Front Genet doi: 10.3389/fgene.2013.00160.
12. Li H, Durbin R (2009) Fast and accurate short read alignment with Burrows-Wheeler transform. Bioinformatics 25: 1754–1760.
13. McKenna A, Hanna M, Banks E, Sivachenko A, Cibulskis K, et al. (2010) The Genome Analysis Toolkit: a MapReduce framework for analyzing next-generation DNA sequencing data. Genome Res 20: 1297–1303.
14. Wang K, Li M, Hakonarson H (2010) ANNOVAR: functional annotation of genetic variants from high-throughput sequencing data. Nucleic Acids Res 38: e164.
15. Williams SR, Aldred MA, Der Kaloustian VM, Halal F, Gowans G, et al (2010). Haploinsufficiency of HDAC4 causes brachydactyly mental retardation syndrome, with brachydactyly type E, developmental delays, and behavioral problems. Am J Hum Genet 87: 219–228.
16. Kong S, Amos CI, Luthra R, Lynch PM, Levin B, et al. (2000) Effects of cyclin D1 polymorphism on age of onset of hereditary nonpolyposis colorectal cancer. Cancer Res 60: 249–252.
17. Zatyka M, da Silva NF, Clifford SC, Morris MR, Wiesener MS, et al (2002). Identification of cyclin D1 and other novel targets for the von Hippel-Lindau tumor suppressor gene by expression array analysis and investigation of cyclin D1 genotype as a modifier in von Hippel-Lindau disease. Cancer Res 62: 3803–3811.
18. Holbrook JA, Neu-Yilik G, Hentze MW, Kulozik AE (2004) Nonsense-mediated decay approaches the clinic. Nat Genet 36: 801–808.
19. Stoller JZ, Epstein JA (2005) Identification of a novel nuclear localization signal in Tbx1 that is deleted in DiGeorge syndrome patients harboring the 1223delC mutation. Hum Mol Genet 14: 885–892.
20. Vezzoli G, Terranegra A, Arcidiacono T, Biasion R, Coviello D, et al. (2007) R990G polymorphism of calcium-sensing receptor does produce a gain-of-function and predispose to primary hypercalciuria. Kidney Int 71: 1155–1162.
21. Ohtani I, Schuknecht HF (1984) Temporal bone pathology in DiGeorge's syndrome. Ann Otol Rhinol Laryngol 93(3 Pt 1): 220–224.
22. Kawame H, Adachi M, Tachibana K, Kurosawa K, Ito F, et al. (2001) Graves' disease in patients with 22q11.2 deletion. J Pediatr 139: 892–895.

Author Contributions

Conceived and designed the experiments: TO YM. Performed the experiments: T. Niihori SN FK MF YA. Analyzed the data: T. Nagashima RF KN. Contributed reagents/materials/analysis tools: KN. Wrote the manuscript: TO. Collected the clinical findings: NT MK.

Gain-of-Function Mutations in *RIT1* Cause Noonan Syndrome, a RAS/MAPK Pathway Syndrome

Yoko Aoki,[1,*] Tetsuya Niihori,[1] Toshihiro Banjo,[2] Nobuhiko Okamoto,[3] Seiji Mizuno,[4] Kenji Kurosawa,[5] Tsutomu Ogata,[6] Fumio Takada,[7] Michihiro Yano,[8] Toru Ando,[9] Tadataka Hoshika,[10] Christopher Barnett,[11,12] Hirofumi Ohashi,[13] Hiroshi Kawame,[14] Tomonobu Hasegawa,[15] Takahiro Okutani,[16] Tatsuo Nagashima,[17] Satoshi Hasegawa,[18] Ryo Funayama,[19] Takeshi Nagashima,[19] Keiko Nakayama,[19] Shin-ichi Inoue,[1] Yusuke Watanabe,[2] Toshihiko Ogura,[2] and Yoichi Matsubara[1,20]

RAS GTPases mediate a wide variety of cellular functions, including cell proliferation, survival, and differentiation. Recent studies have revealed that germline mutations and mosaicism for classical RAS mutations, including those in *HRAS*, *KRAS*, and *NRAS*, cause a wide spectrum of genetic disorders. These include Noonan syndrome and related disorders (RAS/mitogen-activated protein kinase [RAS/MAPK] pathway syndromes, or RASopathies), nevus sebaceous, and Schimmelpenning syndrome. In the present study, we identified a total of nine missense, nonsynonymous mutations in *RIT1*, encoding a member of the RAS subfamily, in 17 of 180 individuals (9%) with Noonan syndrome or a related condition but with no detectable mutations in known Noonan-related genes. Clinical manifestations in the *RIT1*-mutation-positive individuals are consistent with those of Noonan syndrome, which is characterized by distinctive facial features, short stature, and congenital heart defects. Seventy percent of mutation-positive individuals presented with hypertrophic cardiomyopathy; this frequency is high relative to the overall 20% incidence in individuals with Noonan syndrome. Luciferase assays in NIH 3T3 cells showed that five RIT1 alterations identified in children with Noonan syndrome enhanced ELK1 transactivation. The introduction of mRNAs of mutant *RIT1* into 1-cell-stage zebrafish embryos was found to result in a significant increase of embryos with craniofacial abnormalities, incomplete looping, a hypoplastic chamber in the heart, and an elongated yolk sac. These results demonstrate that gain-of-function mutations in *RIT1* cause Noonan syndrome and show a similar biological effect to mutations in other RASopathy-related genes.

RAS GTPases are monomeric G proteins with a molecular mass of 20–40 kDa and cycle between a GTP-bound active and a GDP-bound inactive state. The members of the RAS superfamily are structurally classified into at least five subfamilies: RAS, Rho, Rab, Sar1/Arf, and Ran families.[1,2] The Ras subfamily consists of classical RAS proteins (HRAS, KRAS, and NRAS), RRAS, RRAS2 (TC21), RRAS3 (MRAS), RAPs, RAEB, RALs, RIT1, and RIT2 (RIN). RAS proteins interact with multiple effectors, including RAF kinases, phosphatidylinositol 3-kinase (PI-3 kinase), RalGDS, p120GAP, MEKK1, RIN1, AF-6, phospholipase C epsilon, and the Nore-MST1 complex, and activate multiple downstream signaling cascades.[1,2] Of these signaling pathways, the RAS/mitogen-activated protein kinase (RAS/MAPK) signaling pathway plays a central role in cellular proliferation and differentiation.

Noonan syndrome (MIM 163950) is an autosomal-dominant disorder characterized by short stature, distinctive facial features, and congenital heart defects.[3,4] The distinctive facial features include hypertelorism, downslanting palpebral fissures, ptosis, a webbed or short neck, and low-set, posteriorly rotated ears. Congenital heart defects, including pulmonary valve stenosis and atrial septal defects, occur in 50%–80% of individuals. Hypertrophic cardiomyopathy is observed in 20% of affected individuals. Other clinical manifestations include cryptorchidism, mild intellectual disability, bleeding tendency, and hydrops fetalis. The incidence of this syndrome is estimated to be between 1 in 1,000 to 1 in 2,500 live births. Individuals with Noonan syndrome are at risk of juvenile myelomonocytic leukemia (JMML), a myeloproliferative disorder characterized by excessive production of myelomonocytic cells.[4] Noonan syndrome exhibits phenotypic overlap

[1]Department of Medical Genetics, Tohoku University School of Medicine, Sendai 980-8574, Japan; [2]Department of Developmental Neurobiology, Institute of Development, Aging, and Cancer, Tohoku University, Sendai 980-8575, Japan; [3]Department of Medical Genetics, Osaka Medical Center and Research Institute for Maternal and Child Health, Izumi 594-1101, Japan; [4]Department of Pediatrics, Central Hospital, Aichi Human Service Center, Kasugai 480-0392, Japan; [5]Division of Medical Genetics, Kanagawa Children's Medical Center, Yokohama 232-8555, Japan; [6]Department of Pediatrics, Hamamatsu University School of Medicine, Hamamatsu 431-3192, Japan; [7]Department of Medical Genetics, Kitasato University Graduate School of Medical Sciences, Sagamihara 252-0373, Japan; [8]Department of Pediatrics, Akita University School of Medicine, Akita 010-8543, Japan; [9]Department of Pediatrics, Municipal Tsuruga Hospital, Tsuruga 914-8502, Japan; [10]Department of Pediatrics, Tottori Prefectural Central Hospital, Tottori 680-0901, Japan; [11]South Australian Clinical Genetics Service, SA Pathology, Women's and Children's Hospital, North Adelaide, Adelaide, SA 5006, Australia; [12]School of Paediatrics and Reproductive Health, University of Adelaide, Adelaide, SA 5005, Australia; [13]Division of Medical Genetics, Saitama Children's Medical Center, Saitama 339-8551, Japan; [14]Department of Genetic Counseling, Ochanomizu University, Tokyo 112-8610, Japan; [15]Department of Pediatrics Keio University School of Medicine, Tokyo 160-8582, Japan; [16]Division of Neonatal Intensive Care Unit, General Perinatal Medical Center, Wakayama Medical University, Wakayama 641-8510, Japan; [17]Department of Pediatrics, Jikei University School of Medicine, Tokyo 105-8461, Japan; [18]Department of Pediatrics, Niigata Graduate School of Medical and Dental Sciences, Niigata 951-8510, Japan; [19]Division of Cell Proliferation, United Centers for Advanced Research and Translational Medicine, Tohoku University Graduate School of Medicine, Sendai 980-8575, Japan; [20]National Research Institute for Child Health and Development, Tokyo 157-8535, Japan
*Correspondence: aokiy@med.tohoku.ac.jp
http://dx.doi.org/10.1016/j.ajhg.2013.05.021.

with Costello syndrome (MIM 218040) and cardiofaciocutaneous (CFC) syndrome (MIM 115150).

In 2001, Tartaglia et al. identified missense mutations in protein-tyrosine phosphatase, nonreceptor type 11 (*PTPN11* [MIM 176876]), which encodes the tyrosine phosphatase SHP-2 in 50% of individuals with Noonan syndrome.[5] In contrast, loss-of-function or dominant-negative mutations in *PTPN11* have been reported in individuals with Noonan syndrome with multiple lentigines[6] (formerly referred to as LEOPARD [multiple lentigines, electrocardiographic conduction abnormalities, ocular hypertelorism, pulmonic stenosis, abnormal genitalia, retardation of growth, and sensorineural deafness] syndrome [MIM 151100]). To date, germline mutations in *PTPN11*, *KRAS* (MIM 190070), *SOS1* (MIM 182530), *RAF1* (MIM 164760), and *NRAS* (MIM 164790) have been identified in individuals with Noonan syndrome[7–12] (NS1 [MIM 163950], NS3 [MIM 609942], NS4 [MIM 610733], NS5 [MIM 611553], and NS6 [MIM 613224]), and mutations in *SHOC2* (MIM 602775) and *CBL* (MIM 165360) have been identified in two Noonan-syndrome-like syndromes[13–16] (NSLH [MIM 607721] and NSLL [MIM 613563], respectively) (Figure S1, available online). Moreover, we and another group have identified germline mutations in *HRAS* (MIM 190020) in individuals with Costello syndrome[17] and germline mutations in *KRAS*, *BRAF* (MIM 164757), *MAP2K1* (MIM 176872), and *MAP2K2* (MIM 601263) in individuals with CFC syndrome.[18,19] Mutations in *BRAF* have been also identified in a small percentage of individuals with Noonan syndrome (NS7 [MIM 613706]). A line of studies have shown that a group of the above genetic disorders result from dysregulation of the RAS and downstream signaling cascade (RAS/MAPK pathway syndromes, or RASopathies).[20,21] Recently, mosaicism for *KRAS* and *HRAS* mutations has been reported in nevus sebaceous and Schimmelpenning syndrome,[22] further extending a spectrum of diseases with a dysregulated RAS/MAPK pathway.

To identify genetic causes of Noonan syndrome, we recruited 180 individuals with Noonan syndrome or a related phenotype; they were negative for all coding exons in *PTPN11*, *KRAS*, *HRAS*, and *SOS1*; exons 6 and 11–16 in *BRAF*; exons 7, 14, and 17 in *RAF1*; exons 2 and 3 in *MAP2K1* and *MAP2K2*; and exon 1 in *SHOC2*. Further genetic analysis has been conducted according to their first diagnoses.[17,23–29] This study was approved by the ethics committee of Tohoku University School of Medicine. We obtained informed consent from all subjects involved in the study. We sequenced the exomes of 14 individuals whose clinical manifestations had been confirmed to be consistent with Noonan syndrome by trained dysmorphologists. Targeted enrichment was performed with the Agilent SureSelect Human All Exon v.1 Kit for four individuals and with the SureSelect Human All Exon 50Mb kit for ten individuals. Exon-enriched DNA libraries from these 14 individuals were sequenced on the Illumina Hiseq 2000 for 91 bp (v.1 kit) or 101 bp (50Mb kit). The Burrows-Wheeler Aligner (BWA) was used to align the sequence reads to the human genome (UCSC Genome Browser hg19);[30] all BWA parameters were kept at the default settings. After the removal of duplicates from the alignments, realignment around known indels, recalibration, and SNP and indel calling were performed with the Genome Analysis Toolkit (v.1.5).[31] ANNOVAR was used for annotation against the RefSeq database and dbSNP.[32] We identified approximately 10,000 nonsynonymous, nonsense, and splice-site variations and coding indels per individual (Table S1). Filtering steps using variant databases (dbSNP132 and the 1000 Genome Project database) and in-house exome data were carried out, resulting in the identification of 122–282 variants per individual. By visual inspection of the generated data, four heterozygous *RIT1* (MIM 609591; RefSeq accession number NM_006912.5) variants (c.246T>G [p.Phe82Leu], c.265T>C [p.Tyr89His], c.270G>T [p.Met90Ile], and c.284G>C [p.Gly95Ala]) were found in four individuals. Sanger sequencing validated the heterozygous state of the four variants. We did not find any other strong candidate genes in the results of exome sequencing.

RIT1 shares approximately 50% sequence identity with RAS, has an additional N-terminal extension, and does not possess a C-terminal CAAX motif, a specific motif for post-translational modification.[33,34] *RIT1* is located in chromosomal region 1q22 and consists of six exons. We analyzed an additional 166 individuals diagnosed with Noonan syndrome or a related disorder but without mutations in known genes.[17,23–29] Sanger sequencing of all coding exons in *RIT1* in the 166 individuals showed that 13 in 166 individuals had changes. Combining with the 4 in 14 individuals from exome sequencing, a total of nine missense, nonsynonymous mutations were identified in 17 of 180 (9%) individuals who were suspected to have Noonan syndrome or a related disorder (Table 1 and Figures 1A–1L). The identified germline *RIT1* mutations encode alterations located in the G1 domain (c.104G>C [p.Ser35Thr]); the switch I region, involving the G2 domain (c.170C>G [p.Ala57Gly]); and the switch II region, corresponding to RAS (c.242A>G [p.Glu81Gly], c.244T>G [p.Phe82Val], c.246T>G [p.Phe82Leu], c.247A>C [p.Thr83Pro], c.265T>C [p.Tyr89His], c.270G>T [p.Met90Ile], and c.284G>C [p.Gly95Ala]) (Figure S2). Amino acids where alterations are located are conserved among species (Figure S3). The *RIT1* mutations encode alterations clustered in the switch II region. In contrast, *HRAS* germline mutations identified in Costello syndrome are clustered at codon 12 and 13 in the region encoding the G1 domain[17] (Figure 1M). Mutations in parents were not identified in seven families. These mutations are apparently de novo, but biologic confirmation of parentage was not performed. One mutation, c.104G>C, was inherited from a mother with a Noonan syndrome phenotype (Table 1). None of these mutations were identified in 480 controls.

To assess the functional consequences of *RIT1* mutations identified in affected individuals, we introduced a

Table 1. Mutations in *RIT1*, Family Status, and Heart Defects of Mutation-Positive Individuals

Subject	Exon	Nucleotide Change[a]	Amino Acid Change[b]	Father	Mother	HCM[c]	PS[c]	Other Heart Defects[c]
NS414	2	c.104G>C	p.Ser35Thr	WT	p.Ser35Thr	+	–	MVP, MR
KCC27	2	c.104G>C	p.Ser35Thr	NA	NA	+	+	–
NS43	4	c.170C>G	p.Ala57Gly	NA	NA	+	–	MR, TR
NS185	4	c.170C>G	p.Ala57Gly	NA	NA	+	+	ASD, PDA
NS216	4	c.170C>G	p.Ala57Gly	NA	NA	+	–	–
NS402	4	c.170C>G	p.Ala57Gly	WT	WT	+	+	–
NS168	5	c.242A>G	p.Glu81Gly	NA	NA	–	+	VSD
NS410	5	c.244T>G	p.Phe82Val	WT	WT	+	–	–
NS358	5	c.246T>G	p.Phe82Leu	WT	WT	–	+	ASD
NS465	5	c.246T>G	p.Phe82Leu	NA	NA	–	+	VSD
NS276	5	c.247A>C	p.Thr83Pro	WT	WT	+	+	PVC
KCC8	5	c.265T>C	p.Tyr89His	NA	NA	+	+	–
KCC38	5	c.270G>T	p.Met90Ile	WT	WT	+	+	ASD, VSD, PDA
NS234	5	c.284G>C	p.Gly95Ala	WT	WT	–	–	ASD
NS265	5	c.284G>C	p.Gly95Ala	WT	WT	+	+	–
Og22	5	c.284G>C	p.Gly95Ala	NA	NA	–	–	–
Og45	5	c.284G>C	p.Gly95Ala	NA	NA	+	+	ASD

PCR primers used for sequencing are shown in Table S3. Nucleotide changes are not located in CpG dinucleotides, suggesting that they exhibit baseline mutation rates with a phenotypic filtering effect and that only these mutations lead to this phenotype. Abbreviations are as follows: WT, wild-type; HCM, hypertrophic cardiomyopathy; PS, pulmonic stenosis; MVP, mitral valve prolapse; MR, mitral regurgitation; TR, tricuspid regurgitation; ASD, atrial septal defect; PDA, patent ductus arteriosus; VSD, ventricular septal defect; PVC, premature ventricular contraction; and NA, not available.
[a]RefSeq NM_006912.5.
[b]RefSeq NP_008843.1.
[c]HCM and heart anomalies were diagnosed by echocardiography.

single-base substitution (p.Ser35Thr, p.Ala57Gly, p.Glu81Gly, p.Phe82Leu, or p.Gly95Ala) identified in individuals with Noonan syndrome into a pCAGGS expression vector[36] harboring *RIT1* cDNA. As an experimental control, cDNAs harboring *RIT1* c.89G>T (p.Gly30Val), c.104G>C (p.Ser35Asn), and c.236A>T (p.Gln79Leu) and *Braf* c.1910T>A (p.Val637Glu) (RefSeq NM_139294), which corresponds to oncogenic p.Val600Glu in humans, were also generated. RIT1 p.Gly30Val and p.Gln79Leu correspond to oncogenic RAS alterations p.Gly12Val and p.Gln61Leu, respectively. We introduced pFR-luc, pFA2-Elk1, phRLnull-luc, and wild-type (WT) or mutant expression constructs of *RIT1* into NIH 3T3 cells to examine the transcriptional activation by ELK1,[18,33] a transcription factor that is activated by MAPK. The results revealed that compared with the WT cDNA, all *RIT1* mutations exhibited significant activation. RIT1 p.Gln79Leu, followed by p.Gly95Ala, p.Ala57Gly, p.Phe82Leu, and p.Glu81Gly, showed the highest ELK1 transactivation, as also shown in a past study[37] (Figure 2A). The c.104G>C (p.Ser35Thr) substitution was identified in two affected individuals. RIT1 p.Ser35Asn, which corresponds to dominant-negative alteration p.Ser17Asn in RAS, has been used as a dominant-negative substitution in cell experiments.[38] To examine the functional consequence of p.Ser35Thr, identified in affected individuals, we compared the ELK1 transactivation in cells expressing p.Ser35Thr and those expressing p.Ser35Asn. Enhanced ELK1 transactivation was observed in cells expressing p.Ser35Thr, but not in cells expressing p.Ser35Asn (Figure 2B). These results suggest that *RIT1* mutations identified in affected individuals were gain-of-function mutations.

RIT1 is expressed ubiquitously in embryonic and adult tissues.[33,34] *Rit1*-null mice have been shown to grow to adulthood without any apparent abnormalities;[39] hence, physiological roles of RIT1 in development remain unknown. To examine the developmental effect of identified mutations, we introduced mRNA of the WT and three *RIT1* mutations (c.236A>T [p.Gln79Leu], c.242A>G [p.Glu81Gly], and c.284G>C [p.Gly95Ala]) into 1-cell-stage zebrafish embryos and observed the phenotype at 11 hr postfertilization (hpf). An oval-shaped egg sack, a typical manifestation of the gastrulation defect, was observed in embryos expressing RIT1 alterations (Figure 3A). This characteristic shape change was also observed in zebrafish expressing gain-of-function mutations of human *NRAS*[40]. Next, we observed the phenotype at later stages (48–52 hpf) (Figure 3B and Figure S4). The introduction of the WT mRNA did not interfere with the normal development, resulting in generally normal morphology

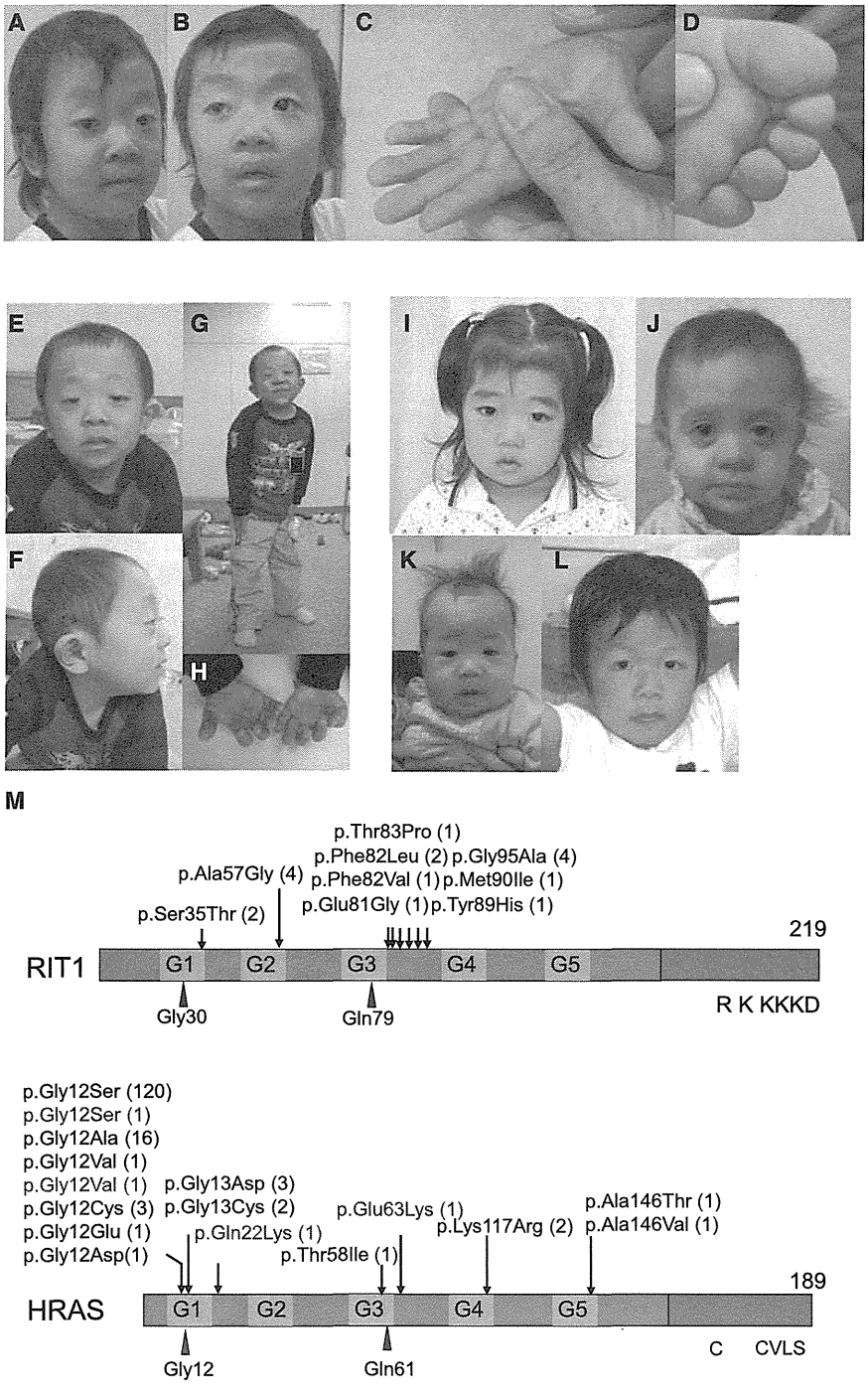

Figure 1. Photographs of Six Individuals in whom *RIT1* Mutations Were Identified
(A–D) KCC38 at 3 years of age. Broad forehead, sparse eyebrows, ptosis, hypertelorism, and hyperpigmentation were observed (A and B). Prominent finger pads were observed (C and D).
(E–H) NS358 at 4 years of age. Hypertelorism, epicanthus, sparse eyebrows, and low-set ears were observed.
(I) NS414 at 3 years of age.
(J) NS465 at 1 year of age.
(K) NS276 at 5 months.
(L) NS265 at 5 years of age.
(M) Structure and identified germline alterations in RIT1 and HRAS. HRAS alterations identified in individuals with Costello syndrome were described before[20] or shown in The RAS/MAPK Syndromes Homepage (see Web Resources). HRAS alterations identified in individuals with congenital myopathy with excess of muscle spindles[35] are indicated in purple.
We obtained specific consent for photographs from six individuals.

in 125/132 (94.7%) embryos; however, 7/132 (5.3%) embryos had limited mild craniofacial and heart abnormalities (Table 2). In contrast, a combined manifestation of craniofacial abnormalities, pericardial edema, and an elongated yolk sac was observed in 66.1%, 52.4%, and 40.5% of embryos expressing p.Gln79Leu, p.Glu81Gly, and p.Gly95Ala, respectively. Development was severely retarded in approximately 7% of embryos expressing RIT1 alterations; these embryos displayed the formation of a disorganized round body shape with a dysmorphic head and body trunk. In the head region, a hypoplastic brain, especially in the telencephalic area, was observed and resulted in misshapen morphology. In the ventral part of the head, the jaw structure was also hypoplastic, and the eyes were translocated medially. These morphological changes gave a cyclopia-like appearance. The ventral sides of the eyes were small, and coloboma along with a loss of pigment was evident (Figure 3B). These phenotypic changes are compatible with the gastrulation defect observed at 11 hpf (Figure 3A). Because the Fgf/Ras/MAPK signaling cascade plays an essential role in the convergent and extension cell movement during gastrulation,[41] perturbation by the RIT1 alterations could cause abnormal cell movement in the axial portions and thus lead to an elongated shape of the egg and the hypoplastic ventral side of the head. Detailed inspection of the morphology in mutant-injected embryos revealed abnormal cardiogenesis, namely, incomplete looping, hypoplastic chambers, and stagnation of blood flow in the yolk sac (Figure 3B). Although the atrium of these hearts beat regularly, the ventricle seemed to twitch passively by the contraction of the atrium (Movies S1, S2, S3, S4, S5, and S6). These results indicate that activating mutations in *RIT1* induce abnormal craniofacial and heart defects in zebrafish.

RIT1-mutation-positive individuals showed a distinct facial appearance, congenital heart defects, and skeletal